ออกไซด์ผสมของแคลเซียม แมกนีเซียมและซิงก์เป็นตัวเร่งปฏิกิริยาวิวิธพันธุ์ชนิดเบสสำหรับ
ทรานส์เอสเทอริฟิเคชันของน้ำมันเมล็ดในปาล์ม

นางสาวศศิพิมพ์ ลิ่มมณี

วิทยานิพนธ์นี้เป็นส่วนหนึ่งของการศึกษาตามหลักสูตรปริญญาวิทยาศาสตรมหาบัณฑิต
สาขาวิชาปิโตรเคมีและวิทยาศาสตร์พอลิเมอร์
คณะวิทยาศาสตร์ จุฬาลงกรณ์มหาวิทยาลัย
ปีการศึกษา 2552

MIXED OXIDES OF Ca, Mg, AND Zn AS HETEROGENEOUS BASE
CATALYSTS FOR TRANSESTERIFICATION OF PALM KERNEL OIL

Miss Sasipim Limmanee

A Thesis Submitted in Partial Fulfillment of the Requirements
for the Degree of Master of Science Program in Petrochemistry and Polymer Science
Faculty of Science
Chulalongkorn University
Academic Year 2009

Thesis Title	MIXED OXIDES OF Ca, Mg, AND Zn AS HETEROGENEOUS BASE CATALYSTS FOR TRANSESTERIFICATION OF PALM KERNEL OIL
By	Miss Sasipim Limmanee
Field of Study	Petrochemistry and Polymer Science
Thesis Advisor	Assistant Professor Chawalit Ngamcharussrivichai, Ph.D.

Accepted by the Faculty of Science, Chulalongkorn University in Partial Fulfillment of the Requirements for the Master's Degree

.... Dean of the Faculty of Science
(Preffessor Supot Hannongbua, Dr.rer.nat.)

THESIS COMMITTEE

.... Chairman
(Professor Patarapan Prasassarakich, Ph.D.)

.... Thesis Advisor
(Assistant Professor Chawalit Ngamcharussrivichai, Ph.D.)

.... Examiner
(Associate Professor Wimonrat Trakarnpruk, Ph.D.)

.... Examiner
(Duangamol Nuntasri, Ph.D.)

.... External Examiner
(Suchada Butnark, Ph.D.)

ศศิพิมพ์ ลิ่มมณี : ออกไซด์ผสมของแคลเซียม แมกนีเซียมและซิงก์เป็นตัวเร่งปฏิกิริยาวิวิธพันธุ์ชนิดเบสสำหรับทรานส์เอสเทอริฟิเคชันของน้ำมันเมล็ดในปาล์ม. (MIXED OXIDES OF Ca, Mg, AND Zn AS HETEROGENEOUS BASE CATALYSTS FOR TRANSESTERIFICATION OF PALM KERNEL OIL) อ.ที่ปรึกษาวิทยานิพนธ์หลัก : ผศ. ดร.ชวลิต งามจรัสศรีวิชัย, 106 หน้า.

วัตถุประสงค์ของงานวิจัยนี้เพื่อศึกษาวิธีการเตรียมตัวเร่งปฏิกิริยาออกไซด์ผสมของแคล-เซียม แมกนีเซียมและซิงก์ด้วยวิธีการตกตะกอนร่วม เพื่อใช้ในการสังเคราะห์ไบโอดีเซลจากปฏิกิริยาทรานส์เอสเทอริฟิเคชันของน้ำมันเมล็ดในปาล์มกับเมทานอล โดยศึกษาปัจจัยที่มีผลต่อลักษณะสมบัติและความสามารถในการเร่งปฏิกิริยาทรานส์เอสเทอริฟิเคชันของตัวเร่งปฏิกิริยา ได้แก่ องค์ประกอบของโลหะในตัวเร่งปฏิกิริยา (Ca:Mg:Zn) อัตราส่วนโดยโมลของคาร์บอเนตต่อโลหะไอออน ความเข้มข้นของสารละลายโซเดียมคาร์บอเนต ความเป็นกรด-เบสของการตกตะกอน เวลาและอุณหภูมิในการบ่ม และอุณหภูมิในการเผา พบว่าตัวเร่งปฏิกิริยาออกไซด์ผสมของแคลเซียม แมกนีเซียม และซิงก์ที่มีอัตราส่วนโดยโมล Ca:Mg:Zn เป็น 3:1:1 ซึ่งเตรียมโดยใช้อัตราส่วนโดยโมลของคาร์บอเนตต่อโลหะไอออนเท่ากับ 1 ความเข้มข้นของสารละลายโซเดียมคาร์บอเนตเท่ากับ 0.75 โมลาร์ สังเคราะห์ที่ pH เท่ากับ 7 บ่มที่อุณหภูมิ 60 องศาเซลเซียสเป็นเวลา 20 ชั่วโมง และผ่านการเผาที่อุณหภูมิ 800 องศาเซลเซียสเป็นเวลา 2 ชั่วโมง เป็นตัวเร่งปฏิกิริยาที่เหมาะสมที่สุด ให้ร้อยละเมทิลเอสเทอร์สูงที่สุด 98 ภาวะที่เหมาะสมในการเร่งปฏิกิริยาทรานส์เอสเทอริฟิเคชันของน้ำมันเมล็ดในปาล์ม คือ ปริมาณตัวเร่งปฏิกิริยาร้อยละ 6 โดยน้ำหนักเทียบกับน้ำหนักน้ำมัน อัตราส่วนโดยโมลของเมทานอลต่อน้ำมัน เป็น 20 อุณหภูมิ 60 องศาเซลเซียส เวลา 3 ชั่วโมง

สาขาวิชาปิโตรเคมีและวิทยาศาสตร์พอลิเมอร์	ลายมือชื่อนิสิต ศศิพิมพ์ ลิ่มมณี
ปีการศึกษา..........2552..........	ลายมือชื่ออ.ที่ปรึกษาวิทยานิพนธ์หลัก

507 24837 23 : MAJOR PETROCHEMISTRY AND POLYMER SCIENCE
KEYWORDS : MIXED OXIDES, TRANSESTERIFICATION

SASIPIM LIMMANEE : MIXED OXIDES OF Ca, Mg, AND Zn AS HETEROGENEOUS BASE CATALYSTS FOR TRANSESTERIFICA-TION OF PALM KERNEL OIL. THESIS ADVISOR : ASST.PROF. CHAWALIT NGAMCHARUSSRIVICHAI, Ph.D., 106 pp.

The objective of this research work is to study the preparation of CaMgZn mixed oxides by co-precipitation. The mixed oxides were applied as a catalyst to transesterification of palm kernel oil with methanol. The parameters influencing the mixed oxide characteristics and transesterification performance were studied including metal composition (Ca:Mg:Zn), molar ratio of CO_3^{2-} to metal ion, CO_3^{2-} concentration, pH during precipitation, aging time, aging temperature, and calcination temperature. The results indicated that CaMgZn with the Ca:Mg:Zn molar ratio of 3:1:1, synthesized by using the molar ratio of CO_3^{2-}/metal ion of 1.0, the CO_3^{2-} concentration of 0.75 M, pH of 7, the aging temperature of $60^{\circ}C$, the aging time of 20 h and the calcination temperature of $800^{\circ}C$ for 2 h, exhibited the most active catalyst. The catalyst gave the highest methyl ester content of 98%. The suitable conditions for the transesterification of palm kernel oil were the amount of catalyst of 6 wt.%, the methanol/oil molar ratio of 20, the temperature of $60^{\circ}C$ and the reaction time of 3 h.

Field of Study : Petrochemistry and Polymer Science   Student's Signature Sasipim Limmanee

Academic Year :   2009   Advisor's Signature Chawalit N.

ACKNOWLEDGEMENTS

ศูนย์วิทยทรัพยากร
จุฬาลงกรณ์มหาวิทยาลัย

CONTENTS

PAGE

LIST OF TABLES

LIST OF FIGURES

LIST OF ABBREVIATIONS

°C	: Degree Celsius
cm	: Centimeter
g	: Gram
h	: Hour
l	: Liter
M	: Molar
mol	: Mole
ml	: Milliliter
wt.%	: Weight Percentage
µm	: Micrometer

CHAPTER I

INTRODUCTION

1.1 The Statement of Problem

The fossil fuels mainly crude oil, natural gas and coal have been playing an important role worldwide as the major energy resources. In recent years, the energy demand is increasing continuously because of the growth of population and the rapid development of industry and economics. Diesel fuel is a petroleum-based fuel, largely utilized in the area of transportation, agriculture, power generation and industries. However, the petroleum sources are limited and non-renewable. Moreover, the petroleum-derived fuels contain aromatics, organic sulfurs, and heavy metals. Their combustion emitts pollutants in the form of oxides of sulfur, oxides of carbon, particulate matter and unburnt hydrocarbons. Therefore, there is an urgent need to develop alternative fuels that are renewable, clean and economically feasible as a substitute to the petroleum diesel.

Biodiesel is a mixture of monoalkyl esters of long chain fatty acids derived from renewable feedstocks such as vegateble oils or animal fats [1]. It can be used directly in diesel engines without requiring engine modifications. Biodiesel is usually produced by transesterification of vegetable oils or animal fats with a monoalkyl alcohol (methanol or ethanol) in the presence of a catalyst. The catalysts most frequently used in the industrial biodiesel production are homogeneous basic catalysts, for example NaOH and KOH. The base-catalyzed transesterification can actively produce monoalkyl esters with a high yield under mild conditions. However, in the homogeneous process, removal of the soluble catalysts from the reaction mixture is difficult and generates a large amount of alkali wastewater during washing step.

Heterogeneous catalysts can overcome these problems since they can be easily separated from the reaction mixture and reutilized, diminishing waste from the conventional process. A number of heterogeneous base catalysts for the transesterification of vegetable oils such as Na/NaOH/γ-Al$_2$O$_3$ [2] and various alkali metal compounds supported on alumina [3-5] have been proposed. However, since the active oxide species are easily leached by methanol, the supported alkali catalysts exhibited short service lifetime [6]. Several oxides of alkali earth metals such as CaO [7-11] and MgO [12-14] have been investigated to minimize the leaching effect due to their low solubility in methanol [7]. The mixed metal oxides have gain attention because of their improved basicity. It is established that the mixed oxide of Ca and Zn with the Ca/Zn ratio of 0.25 was active in the methanolysis of palm kernel oil [15]. This result emphasizes the advantage of co-existence of two different basic oxide components in the catalyst for transesterification.

The present thesis is an attempt to improve the physicochemical properties and the catalytic performance of the mixed oxides based on Ca and Zn for the transesterification of palm kernel oil. An introduction of magnesium into the mixed oxide is supposed to increase the basic properties, leading to an enhancement of the activity of the resultant mixed oxides. We have prepared the mixed oxides of Ca, Mg and Zn by pH-controlling co-precipitation method. Effects of various factors such as metal composition, aging time and aging temperature were studied to find suitable conditions for the catalyst preparation. The physicochemical properties of the mixed oxides were investigated by several techniques. The catalytic performance was studied in the transesterification of palm kernel oil with methanol under batch conditions. Moreover, the influences of reaction conditions on methyl ester (ME) content were investigated.

1.2 Objectives of the Research Work

1. To synthesize mixed oxides of Ca, Mg and Zn by pH-controlling precipitation method.

2. To study the transesterification of palm kernel oil with methanol over the prepared mixed oxides of Ca, Mg and Zn.

1.3 Scope of the Research Work

1. Literature survey.

2. Synthesize mixed oxides of Ca, Mg and Zn by pH-controlling co-precipitation method. The parameters influencing the physical properties and transesterification performance of the resultant catalysts are studied, including.

- Metal composition (Ca:Mg:Zn)   0:1:1, 1:1:1, 3:1:1, 1:3:1 and 1:1:3
- Molar ratio of CO_3^{2-} to metal ion   0.75-1.5
- Sodium carbonate concentration   0.5-1 M
- pH during precipitation   7, 8, 9 and 10
- Aging time   8 and 20 h
- Aging temperature   room temperature and 60°C
- Calcination temperature   500, 600, 700 and 800°C

3. Find the suitable conditions for the catalyst preparation.

4. Characterize the prepared catalysts by following techniques:

- Scanning electron microscopy (SEM)
- X-ray fluorescence spectrometry (XRF)
- X-ray diffraction (XRD)
- N_2 adsorption-desorption measurement
- Thermogravimetric and differential thermal analysis (TG/DTA)
- Temperature-programmed desorption of CO_2 (CO_2-TPD)

5. Study effects of transesterification conditions on the formation of methyl esters. Various reaction parameters are investigated, including methanol/oil ratio, catalyst

amount and reaction time. The methyl ester (ME) content in the biodiesel product is determined by gas chromatography.

6. Summarize the results and write thesis.

CHAPTER II

THEORY AND LITERATURE REVIEWS

2.1 Biodiesel

Biodiesel is defined as a mixture of monoalkyl esters of long chain fatty acids derived from renewable feedstocks, such as vegetable oils or animal fats. Biodiesel has a potential to be an alternate for conventional diesel fuel produced from crude oil. It can be used directly as fuel or blended with petroleum diesel and used in diesel engines with few or no engine modifications. Neat biodiesel fuel is designated as B100. A biodiesel blend is a mixture of pure biodiesel with the conventional diesel. For example, B20 is derived from 80 vol.% petroleum diesel blended with 20 vol.% B100. Advantages of biodiesel are the following:

- It is made from renewable sources that can be produced domestically.
- It reduces emission of carbon monoxide, sulfur dioxide, unburnt hydrocarbons and particulate matters generated during the combustion process.
- It has relatively high cetane number and high lubricant properties compared to diesel fuel.
- It has no aromatics and sulfur compounds.
- It contains high oxygen by weight, which improves the combustion process
- It is biodegradable and non toxic.

2.1.1 Properties of biodiesel

Biodiesel is a clear yellow liquid with a viscosity similarly to that of petrodiesel. Typically, it comprises of esters with long chain fatty acids of C_{12}-C_{22} and short chain alkyl alcohols. Table 1 compares some important properties of diesel and biodiesel. As can be seen, the physicochemical properties of biodiesel are similar to diesel fuel. However, the fuel properties of biodiesel are superior to those of diesel

fuel. Biodiesel has a higher flash point, meaning a safe handling and transporting. It possesses the oxygen content of ca. 11 wt.% of oxygen by weight, which enhances a complete combustion in an engine. Moreover, it possesses high cetane number corresponds to shorter ignition delay time and advances the combustion timing.

Table 2.1 Comparison of diesel and biodiesel properties [16]

Property	Diesel	Biodiesel
Composition	Hydrocarbon $(C_{10}\text{-}C_{21})$	Fatty acid alkyl ester $(C_{12}\text{-}C_{22})$
Kinematic viscosity range $(mm^2s^{-1}$, at 313 K)	1.3-4.1	1.9-6.0
Specific gravity $(g^{-1}ml)$	0.85	0.88
Flash point range (K)	333-353	373-443
Cloud point range (K)	258-278	270-285
Pour point range (K)	243-258	258-289
Water (vol.%)	0.05	0.05
Carbon (wt.%)	87	77
Hydrogen (wt.%)	13	12
Oxygen (wt.%)	0	11
Sulfur (wt.%)	0.05	0.05
Cetane number range	40-55	48-60

2.1.2 Quality specifications of biodiesel

Prior to use biodiesel as a commercial fuel, its physicochemical and fuel properties must be analyzed to ensure the standard specifications required. In the United States, biodiesel must meet the specifications issued by the American Society of Testing and Materials (ASTM). ASTM D 6751 is the method for verifying pure biodiesel, while biodiesel blends cointaining B100 in the range of 6 to 20 wt.% are

tested according to ASTM D 7467. EN 14214 is the standard biodiesel used in the European countries. In the United Kingdom, it is known as BS EN 14214, while DIN EN 14214 is set in Germany. In Thailand, the biodiesel properties are evaluated according to the standard issued by Department of Energy Business, Ministry of Energy, which is adopted from the ASTM and EN standards. The standard specification for biodiesel in Thailand is listed in Table 2.2.

Table 2.2 Standard specification for biodiesel in Thailand [17]

Property	Lower limit	Upper limit	Test method
Methyl ester (wt.%)	96.5	-	EN 14103
Density at 15°C (kg l^{-1})	860	900	ASTM D 1298
Viscosity at 40°C (cSt)	3.5	5	ASTM D 445
Flash point (°C)	120	-	ASTM D 93
Sulphur (wt.%)	-	0.0010	ASTM D 2622
Carbon residue, on 10% distillation residue (wt.%)	-	0.30	ASTM D 4530
Cetane number	51	-	ASTM D 613
Sulfated ash (wt.%)	-	0.02	ASTM D 874
Water (wt.%)	-	0.050	ASTM D 2709
Total contaminate (wt.%)	-	0.0024	ASTM D 5452
Copper strip corrosion	-	No.1	ASTM D 130
Oxidation stability at 110°C (hours)	-	6	EN 14112
Acid value (mg $_{KOH}$ g^{-1})	-	0.50	ASTM D 664
Iodine value (g $_{I2}$100 g^{-1})	-	120	EN 14111
Linolenic acid methyl ester (wt.%)	-	12	EN 14103
Methanol (wt.%)	-	0.20	EN 14110

Table 2.2 Standard specification for biodiesel in Thailand [17] (continued)

Property	Lower limit	Upper limit	Test method
Monoglyceride (wt.%)	-	0.80	EN 14105
Diglyceride (wt.%)	-	0.20	EN 14105
Triglyceride (wt.%)	-	0.20	EN 14105
Free glycerin (wt.%)	-	0.02	EN 14105
Total glycerin (wt.%)	-	0.25	EN 14105
Group I metals (Na+K) (mg kg^{-1})	-	5.0	EN 14108 and EN 14109
Group II metals (Ca+Mg) (mg kg^{-1})	-	5.0	pr EN 14538
Phosphorus (wt.%)	-	0.0010	pr EN 14538

The parameters used to define the quality of biodiesel can be divided in to two groups. One of them is set for determination of the fuel properties similarly to those of petrodiesel, whereas the other describes the chemical composition and impurity remaining. The former includes, for example, density, viscosity, flash point, sulfur content, carbon residue, cetane number and sulfated ash. The latter comprises of, for example, methyl ester content, water content, free glycerin, total glycerin and methanol content. The definition of these parameters is described below:

- **Methyl ester content**

Methyl ester content is related to the methyl ester concentration (wt.%) in biodiesel. Analytical method for evaluation of the methyl ester content is based on a gas chromatography according to the European standard EN 14103. Lower methyl ester content values indicate the presence of wisher amount of mono-, di- and triglyceride than the methyl ester. The viscosity of biodiesel is increased as the amount of mono-, di- and triglycerides increases. An increase in the viscosity affects the fluidity of the biodiesel, which can lead to the formation of engine deposit.

- **Density at 15°C**

Density can be defined as the mass per unit volume of any liquid at a given temperature. Diesel injection equipment meters the fuel by volume. A change in the fuel density influences the engine output power due to a different mass of injected fuel [18]. The density of the fuel also affects injection timing, injection pressure and fuel spray characteristics. Therefore, the density has a strong influence on the engine performance. In addition, the fuel density affects the exhaust emissions. There is a correlation between the fuel density and the emission of particulate matter (PM) and NO_x. The higher density leads to the larger amount of PM and NO_x released [19]. The density of biodiesel depends on the fatty acid composition and impurities. Although biodiesel exhibits higher density than the conventional of diesel, it possesses lower energy content on both a mass and a volume basis. It means that more volume of biodiesel is required to inject into the combustion chamber in order to gain the same power from the engine, resulting in higher fuel consumption.

- **Viscosity at 40°C**

Viscosity has a significant impact on the operation of engine fuel injection and atomization systems. A high viscosity interfere the injection process leading to insufficient fuel atomization. Moreover, the fuel with higher viscosity can cause an early injection due to a high line pressure, which moves the combustion zone closer to top dead center, increasing the maximum pressure and temperature in the combustion chamber [20]. On the other hand, a leakage in the fuel system can be found when the fuel with low viscosity is applied. Viscosity of any fuel is related to its chemical structures. For biodiesel, it is influenced by several factors such as fatty acid chain length, degree of unsaturation (number of double bonds), which depends on the fatty acid composition of the starting oil or fat. An increase in the carbon chain length and number of double bonds results in an increase in the viscosity [21].

- **Flash point**

A key property determining the flammability of a fuel is the flash point. The flash point is the lowest temperature at which the fuel starts to burn when it comes to contact with fire. This temperature is correlated with its volatility, which affects the

starting and warming of engine [20].The flash point of biodiesel is higher than that of diesel fuel. Although this property does not directly influence the combustion, it concerns more safety in the handling, storage and transportation. Methanol remaining in biodiesel reduces the flash point of biodiesel. ASTM D 93 limits the methanol content in the biodiesel fuel to a maximum of about 0.2% (w/w).

- **Sulfur content**

Sulfur content is a weight percentage of sulfur element in a fuel. Sulfur is set according to an environmental concern, since sulfur is converted to SO_x (SO_2 and SO_3) during the fuel combustion. SO_x poisons the catalytic converter and generates acid rain. Biodiesel contains little or no sulfur, while petrodiesel possesses high sulfur levels. Therefore, the use of biodiesel instead of the conventional diesel reduces the SO_x emission. According to ASTM D 2622, the maximum sulfur content in biodiesel must be less than 0.0010 wt.%.

- **Carbon residue**

Carbon residue is a measure of amount of carbon remaining after combustion. It corresponds to the contents of glycerides, free fatty acid, soaps, residual catalysts and other impurities [22]. The carbon residue is an important parameter for diesel engines due to the possibility of carbon residues clogging the fuel injectors.

- **Cetane number**

Cetane number is a measure of ignition quality or ignition delay, and is related to the time required for ignition of a liquid fuel after being injected into a compression-ignition engine [23]. The higher the cetane number is the shorter the ignition delay and the better the ignition quality. The cetane number is determined by following ASTM D 613. A long straight-chain hydrocarbon, hexadecane, is set as a standard for the cetane number of 100, while 2,2,4,4,6,8,8,-heptamethylnonane with a highly branched structure is a standard with the cetane number of 15. Accordingly, it indicates that saturated straight-chain hydrocarbons have higher cetane number than branched-chain or aromatic compounds. The cetane number of biodiesel depends on the distribution of fatty acids in the starting oil or fat. The longer the fatty acid carbon

chains and the higher the degree of saturation are present in the oil or fat, the higher the cetane number of biodiesel product is attained [24].

- **Sulfated ash**

    Sulfated ash is a residue remaining after a fuel sample is carbonized. The standard specification for measurement of sulfated ash is ASTM D 874. This property is an important indicator of quantity of residual metals in biodiesel that is derived from the catalyst used in the transesterification. The high content of ash in the fuel leads to engine deposits and high abrasive wear levels.

- **Water content**

    Water is a major source of fuel contamination. The presence of high level of water content in biodiesel causes many problems. Water causes corrosion of components in engine fuel system. The other problem is that water promotes microbial growth. There are various species of yeast, fungi, and bacteria growing at the fuel-water interface. These organisms produce sludges and slimes resulting in a filter plugging.

- **Total contaminants**

    The presence of contaminants such as unsaponifiable matter, free fatty acids, soap and residual catalyst can affect the quality of biodiesel. The unsaponifiable matter consists of plant sterols, tocopherols and hydrocarbons with small quantities of pigments and minerals. Most biodiesel is produced using soluble alkaline catalysts such as sodium hydroxide and potassium hydroxide. Free fatty acids that are present will react with the alkaline catalyst to form soaps. However, this contaminant can be removed during washing of biodiesel with water. The problem associated with these contaminants is to reduce the storage stability.

- **Copper strip corrosion**

    Some components in diesel fuel, especially sulfur compounds, are corrosive. The corrosiveness of a fuel has implication on storage and utilization. The copper strip corrosion test is used to evaluate a tendency of the fuel to cause corrosion. It is

therefore a measure of how the fuel is harmful to the copper and brass components of the fuel system. The test is performed on each fuel to evaluate relative degree of corrosivity, and then each strip is compared with the data in ASTM D 130. The classification code, denoted as numbers 1, 2, 3, or 4, represents slight tarnish, moderate tarnish, dark tarnish, or corrosion, respectively [19]. The degree of tarnish on the corrode strip correlates the overall corrosiveness of the fuel sample. However, biodiesel is generally less corrosive than the conventional diesel fuel.

- **Oxidation stability**

Oxidation stability shows resistance of a fuel towards oxidation during an extended storage. EN 14112 is used to evaluate the oxidation stability of biodiesel. The oxidation of biodiesel is related to the presence of double bonds in fatty acid chains. When biodiesel is exposed to oxygen, the oxidation will occur. The oxidation of fatty compounds is a multi-step reaction. The initial species formed during the oxidation process are hydroperoxides, which chemically interact with each other to produce high molecular weight insoluble sediments and gums. In some cases, the oxidized fatty acid chains may split and form aldehydes, ketones and short chain acids [20]. The formation of sediments and gums can cause fuel filter plugging and carbon deposits on the fuel system components [25]. The stability of fatty compounds is affected by several factors such as presence of air, heat, light, metallic contaminants, or chemical structure of the compounds, mainly the presence of double bonds. The oxidation stability decreased with the increase of polyunsaturated fatty acids contents.

- **Acid value**

Acid value is expressed in milligram of KOH required to neutralize 1 gram of fatty acid methyl esters. The maximum value for biodiesel is set and is set of ≤0.5 mg KOH/g according to EN 14214. The acid value is a direct measurement of free fatty acids in biodiesel. Biodiesel with a high content of free fatty acid can be corrosive to storage tank. When water is present, a part of the esters is hydrolyzed to long chain free fatty acids, which increasing the acid value.

- **Iodine value**

Iodine value is an indication of total unsaturation in oil and fatty acid. It is expressed in grams of iodine required for reaction with double bonds containing in 100 grams of the sample. The higher the iodine value is the larger the quantity of double bonds is present. Biodiesel with a low iodine value and therefore low degree of unsaturation, is less sensitive to oxidation process.

- **Linolenic acid methyl ester content**

Linolenic acid methyl ester content (C18:3) is related to degree of unsaturation of biodiesel. The content of linolenic acid methyl ester is determined by EN 14103 due to a tendency of methyl linolenate oxidation (max. 12.0 wt.%). The high content of linolenic acid methyl ester results in polymerization of glycerides, which leads to a formation of deposits and/or a deterioration of lubricating oil [22].

- **Methanol content**

Methanol remaining in biodiesel promotes metal corrosion, especially aluminum, and decreases the flash point of biodiesel. EN 14110 limits the maximum content of methanol in biodiesel at 0.2% (w/w).

- **Mono-,di- and triglycerides content**

Mono-, di- and triglycerides content is an indicator of an incomplete tranesterification reaction. After the transesterification, the resulting product contains not only the desired alkyl esters but also unreacted triglycerides and intermediates. Since transesterification is a stepwise reaction, mono- and diglycerides formed as intermediates can also be found in biodiesel. These contaminants may cause severe operational problems, such as engine deposits, filter clogging, or fuel deterioration.

- **Free and total glycerin content**

Free glycerin, a byproduct from triglyceride transesterification, should not be present when the esters product is washed thoroughly with water. However, glycerin may be found in biodiesel as a result of inappropriate processing, such as insufficient separation of the glycerin phase or insufficient water washing after separation. An

incomplete removal of glycerin provides biodiesel with a high free glycerin and total glycerin. If the free glycerin is too high, the storage tank and the fuel system components can be contaminated. Moreover, the problem of injection fouling is found to relate with a higher content of free glycerin.

- **Group I metals (Na+K) and Group II metals (Ca+Mg) content**

Determination of amount of Na, K, Ca and Mg remaining in biodiesel is important for biodiesel quality control. The conventional biodiesel production process employs NaOH or KOH as the homogeneous catalysts. Residual Na and K may be found in biodiesel due to an insufficient washing and purification. Ca and Mg may be introduced into biodiesel during the purification step through washing with hard water or use of a drying agent (such as magnesium sulfate). These alkali and alkali earth metals can promote ash build-up in the engine engine corrosion.

- **Phosphorus content**

Phosphorus presenting in biodiesel is derived from phospholipids remaining in vegetable oils after refining. It can poison catalytic converter used for reduction of exhaust emissions. The phosphorus content of biodiesel produced in Thailand is measured according to prEN 14538. The maximum phosphorus content is limited to 0.0010 wt.%.

2.2 Vegetable Oils

2.2.1 Chemical composition of vegetable oils

The main constituent of vegetable oils is triglycerides. Vegetable oil comprises of 90 to 98% of triglycerides and small amounts of mono- and diglycerides. A triglyceride molecule is made up of one mole of glycerol and three moles of fatty acids. The reaction for the formation of triglyceride is esterification (Eq.(2.1)).

$$\text{(2.1)}$$
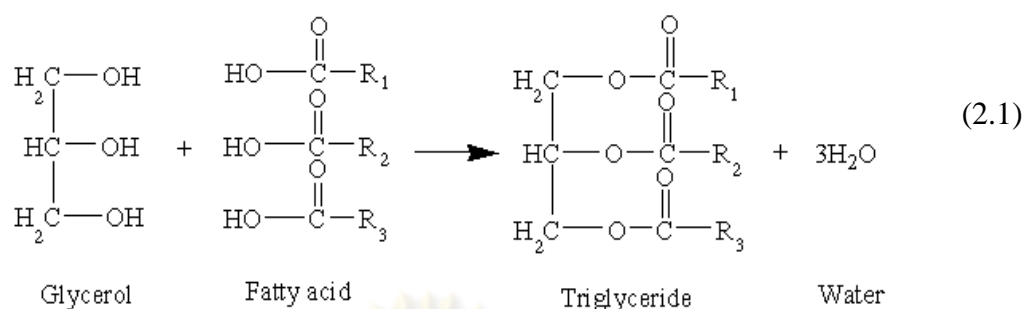
When three fatty acids are identical, the product is a simple triglyceride, whereas a so-called mixed triglyceride consists of dissimilar fatty acids [26]. The terms of monoglyceride or diglyceride refer to the numbers of fatty acids that are attached to the glycerol backbone. Diglyceride has one hydroxyl group and two fatty acid groups attached to the glycerol backbone as shown in Figure 2.1.
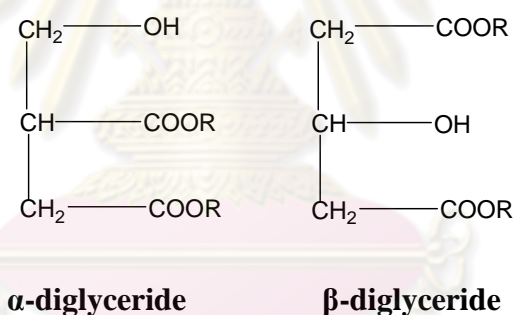
Figure 2.1 Chemical structures of diglyceride.

Fatty acids vary in the number of carbon atoms and double bonds in hydrocarbon chain. They are designated by two numbers separated by a colon. The first number represents the number of carbon atoms in the fatty acid chain and the second number shows the number of double bonds. For example, C18:1 (oleic acid) represents the fatty acid with 18 carbon atoms and 1 double bond. Table 2.3 shows fatty acid composition found in different vegetable oils.

Table 2.3 Fatty acid composition of various vegetable oils [27-29]

Vegetable oil	Composition (wt.%)								
	12:0	14:0	16:0	16:1	18:0	18:1	18:2	18:3	Other
Almond kernel	0	0	6.5	0.5	1.4	70.7	20.0	0	0.9
Bay laurel leaf	26.5	4.5	25.9	0.3	3.1	10.8	11.3	17.6	0
Canola	0	0	4	0	2	61	22	10	1
Castor[a]	0	0	1.1	0	3.1	4.9	1.3	0	89.6
Coconut	0	0	9.7	0.1	3	6.9	2.2	0	65.7
Corn	0	0	6.5	0.6	1.4	65.6	25.2	0.1	0.6
Corn marrow	0	0	11.8	0	2	24.8	61.3	0	0.3
Cottonseed	0	0	28.7	0	0.9	13	57.4	0	0
Hazelnut kernel	0	0	4.9	0.2	2.6	83.6	8.5	0.2	0
Linseed	0	0	5.1	0.3	2.5	18.9	18.1	55.1	0
Grape	0	0.1	6.9	0.1	4	19	69.1	0.3	0.5
Olive	0	0	11.6	1	3.1	75.0	7.8	0.6	0.9
Olive kernel	0	0	5	0.3	1.6	74.7	17.6	0	0.8
Palm	0	0	42.6	0.3	4.4	40.5	10.1	0.2	1.1
Peanut	0	0.1	8	0	1.8	53.3	28.4	0.3	8.1

Table 2.3 Fatty acid composition of various vegetable oils [27-29] (continued)

Vegetable oil	Composition (wt.%)								
	12:0	14:0	16:0	16:1	18:0	18:1	18:2	18:3	Other
Peanut kernel	0	0	11.4	0	2.4	48.3	32.0	0.9	4
Poppyseed	0	0	12.6	0.1	4.0	22.3	60.2	0.5	0
Rapeseed	0	0	3.5	0	0.9	64.1	22.3	8.2	0
Safflower seed	0	0	7.3	0	1.9	13.6	77.2	0	0
Seasameseed	0	0	13.1	0	3.9	52.8	30.2	0	0
Soybean	0	0	13.9	0.3	2.1	23.3	56.2	4.3	0
Sunflowerseed	0	0	6.4	0.1	2.9	17.7	72.9	0	0
Walnut kernel	0	0	7.2	0.2	1.9	18.5	56	16.2	0
Wheat grain	0	0.4	20.6	1.0	1.1	16.6	56	2.6	1.7

[a] Castor oil contains 89.6% ricinoloic acid

2.2.2 Fuel properties of vegetable oils

Fuel properties of vegetable oils are listed in Table 2.4. The kinematic viscosity of vegetable oils varies in the range of 30-40 mm^2s^{-1} which is higher than that of diesel fuel. The high viscosity is resulted from their high molecular weight and chemical structure. The cetane numbers is in the range of 33-50. Vegetable oils posses high flash point (above 200°C). The heating value of vegetable oils (39-40 MJ kg^{-1}) is slightly lower than that of diesel fuel (50 MJ kg^{-1}). The presence of chemically bound oxygen in triglyceride lowers the heating value of vegetable oils.

Table 2.4 Fuel properties of various vegetable oils [29-30]

Vegetable oil	Kinematic viscosity at 38°C $(mm^2\ s^{-1})$	Cetane no.	Heating value $(MJ\ kg^{-1})$	Cloud point (°C)	Pour point (°C)	Flash point (°C)	Density $(kg\ l^{-1})$
Almond kernel	34.2	34.5	39.8	-	-	-	-
Bay laurel leaf	23.2	33.6	39.3	-	-	-	-
Babassu	30.3	38.0	-	20.0	-	150	0.9460
Castor	29.7	42.3	37.4	-	-	-	-
Corn	34.9	37.6	39.5	-1.1	-40.0	277	0.9095
Cottonseed	33.5	41.8	39.5	1.7	-15.0	234	0.9148
Crambe	53.6	44.6	40.5	10.0	-12.2	274	0.9048
Hazelnut kernel	24.0	52.9	39.8	-	-	-	-
Linseed	27.2	34.6	39.3	1.7	-15.0	241	0.9236
Olive kernel	29.4	49.3	39.7	-	-	-	-

Table 2.4 Fuel properties of various vegetable oils [29-30] (continued)

Vegetable oil	Kinematic viscosity at 38°C (mm² s⁻¹)	Cetane no.	Heating value (MJ kg⁻¹)	Cloud point (°C)	Pour point (°C)	Flash point (°C)	Density (kg l⁻¹)
Palm	39.6	42.0	-	31.0	-	267	0.9180
Peanut	39.6	41.8	39.8	12.8	-6.7	271	0.9236
Rapeseed	37.0	37.6	39.7	-3.9	-31.7	246	0.9115
Safflower	31.3	41.3	39.5	18.3	-6.7	260	0.9144
Wheat grain	32.6	35.2	39.3	-	-	-	-
Diesel	3.06	50	43.8	-	-16	76	0.855

2.2.3 Oil plants

Raw material is the major factor affecting selling cost of biodiesel product. The choice of raw materials depends on their availability and cost. Soybean oil is commonly used in the United States, while rapeseed oil is more abundant in the European countries for biodiesel production. In India, Jatropha (*Jatropha Curcus*) [31] and Karanja (*Pongamia pinnata*) [32] is used as the major triglyceride source. The raw materials used at present in Malaysia and Indonesia are coconut oil and palm oils. Currently, the potential raw material for biodiesel production in Thailand is palm oil.

2.2.3.1 Palm oil and palm kernel oil

Palm oil is a potential raw material for biodiesel production in Thailand due to its high crop yield. Palm tree is mainly growing in the south of Thailand. The major area for palm plantation are in three provinces; Krabi, Chumporn and Suratthani. Table 2.5 shows the harvested area of palm oil, amount of palm oil produced and palm oil price between 2003 and 2007. The harvested area has steadily increased from 19,023 hectare in 2003 to 32,718 hectare in 2007 due to the policy of the Thai government. In term of production, Thailand's palm oil production increased from 4,902,575 metric tons in 2003 to 7,378,230 metric tons in 2007.

Table 2.5 Palm oil harvested area, palm oil production and the price of palm oil in Thailand during 2003-2007. [33]

Year	Palm oil harvested area (hectare)			Palm oil production (metric ton)			Price of power crop (baht/metric ton)
	Central	South	Total	Central	South	Total	Palm oil
2003	19,023	268,880	287,903	293,392	4,609,183	4,902,575	2,340
2004	21,062	288,553	309,615	310,358	4,871,439	5,181,797	3,110
2005	22,515	301,677	324,192	311,647	4,691,023	5,002,670	2,760
2006	28,436	351,436	379,872	428,707	5,812,046	6,240,753	2,390
2007	32,718	405,530	438,248	497,508	6,880,722	7,378,230	3,080

Palm oil and palm kernel oil are both derived from the *Elaeis guineensis* palm tree. Its origin is believed to be in the humid forests of East Africa. The palm fruit is oval shaped, about 3-cm long, and looks like a small red plum as shown in Figure 2.2a. The outer fleshy mesocarp gives the viscous orange palm oil while the kernel, which is inside a hard shell, gives the clear white palm kernel oil (Figure 2.2b). Both oils from the same fruit have difference in the fatty acid composition.
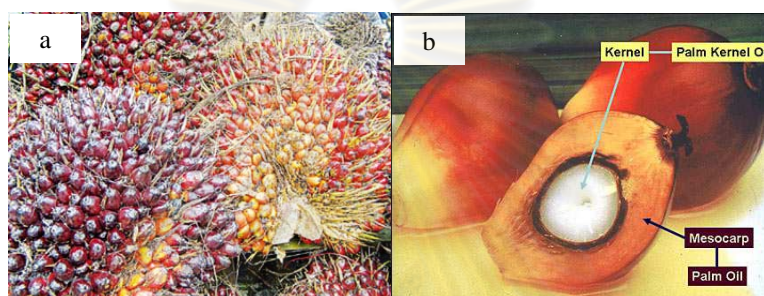
Figure 2.2 Palm bunches (a) and palm fruits (b)

The major acid components of palm oil are palmitic acid (C16:0) and oleic acid (C18:1). Others found with significant amount are linoleic acid (C18:2), stearic acid (C18:0) and myristic acid (C14:0). C_8-C_{12} fatty acids, which may be derived from the endocarp rather than the mesocarp, are present at trace amounts. On the other hand, the major fatty acids in palm kernel oil are lauric acid (C12:0), myristic aicd and oleic acid with the distribution of 45, 16 and 15%, respectively [34].

2.3 Biodiesel Production

2.3.1 Transesterification reaction

Transesterification, also called alcoholysis, is the displacement of alcohol from an ester by another alcohol in a process similar to hydrolysis, except that an alcohol is employed instead of water. The transesterification reaction is represented by the general equation (Eq.(2.2))**.**

$$RCOOR^1 + R^2OH \overset{\text{Catalyst}}{\rightleftharpoons} RCOOR^2 + R^1OH \qquad (2.2)$$

$$\text{Ester} \qquad \text{Alcohol} \qquad\qquad \text{Ester} \qquad \text{Alcohol}$$
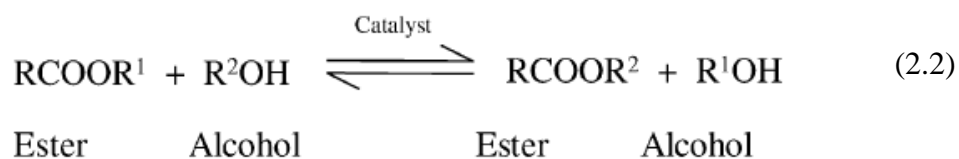
The most commonly preferred method for biodiesel production is transesterification in which a triglyceride molecule is chemically split up by reacting with monohydric alcohol in the presence of a catalyst. In this process, glycerol is taken from the triglyceride and replaced with alkyl radical of the alcohol used in the reaction. Thus, glycerol based triesters are converted to alkyl based monoesters. The general equation for the transesterification of triglyceride with alcohol is expressed in Eq. (2.3).

$$
\begin{array}{lcl}
CH_2{-}OOC{-}R_1 & & R_1{-}COO{-}R \qquad CH_2{-}OH \\
| & & | \\
CH{-}OOC{-}R_2 \;+\; 3ROH & \overset{\text{Catalyst}}{\rightleftharpoons} & R_2{-}COO{-}R \;+\; CH{-}OH \\
| & & | \\
CH_2{-}OOC{-}R_3 & & R_3{-}COO{-}R \qquad CH_2{-}OH
\end{array}
\qquad (2.3)
$$

Triglyceride   Alcohol   Esters   Glycerol
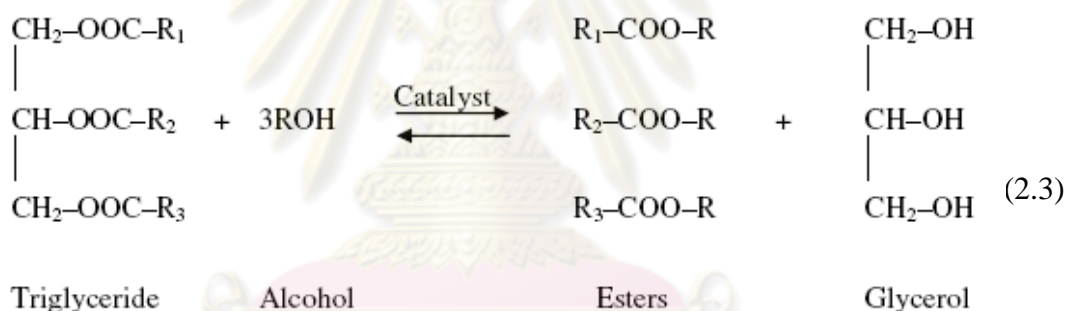
Stoichiometrically, 3 moles of alcohol are required to react with 1 mole of triglyceride. In practice, the high molar ratios of alcohol are needed to shift the equilibrium to achieve a maximum alkyl ester yield.

Basically, transesterification consists of a number of consecutive and reversible reactions as shown in Figure 2.3. The first step is the conversion of triglyceride to diglyceride (Eq.(2.4)), followed by the successive conversion of diglyceride to monoglyceride (Eq.(2.5)), and glycerol (Eq.(2.6)). In each step, an alkyl ester is generated and thus three ester molecules are produced from one molecule of triglyceride.

The conversion of monoglyceride to alkyl ester is believed to be the rate determining step because monoglycerides are the most stable intermediate compound [35].

$$R_1COOCH_2$$
$$|$$
$$R_2COOCH \quad + \quad CH_3OH \quad \xrightleftharpoons[]{\text{Catalyst}} \quad R_2COOCH \quad + \quad R_1COOCH_3 \qquad (2.4)$$
$$|$$
$$R_3COOCH_2 \qquad\qquad\qquad\qquad\qquad R_3COOCH_2$$
$$\textbf{\textit{Triglyceride}} \qquad\qquad\qquad\qquad\qquad \textbf{\textit{Diglyceride}}$$

(with top product $HOCH_2$)

$$HOCH_2 \qquad\qquad\qquad\qquad HOCH_2$$
$$|$$
$$R_2COOCH \quad + \quad CH_3OH \quad \xrightleftharpoons[]{\text{Catalyst}} \quad HOCH \quad + \quad R_2COOCH_3 \qquad (2.5)$$
$$|$$
$$R_3COOCH_2 \qquad\qquad\qquad\qquad R_3COOCH_2$$
$$\textbf{\textit{Diglyceride}} \qquad\qquad\qquad\qquad \textbf{\textit{Monoglyceride}}$$

$$HOCH_2 \qquad\qquad\qquad\qquad HOCH_2$$
$$|$$
$$HOCH \quad + \quad CH_3OH \quad \xrightleftharpoons[]{\text{Catalyst}} \quad HOCH \quad + \quad R_3COOCH_3 \qquad (2.6)$$
$$|$$
$$R_3COOCH_2 \qquad\qquad\qquad\qquad HOCH_2$$
$$\textbf{\textit{Monoglyceride}} \qquad\qquad\qquad\qquad \textbf{\textit{Glycerol}}$$
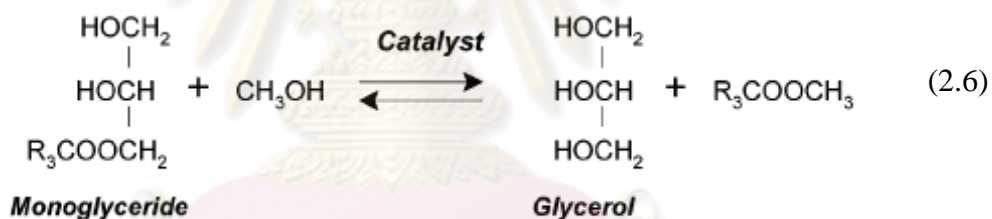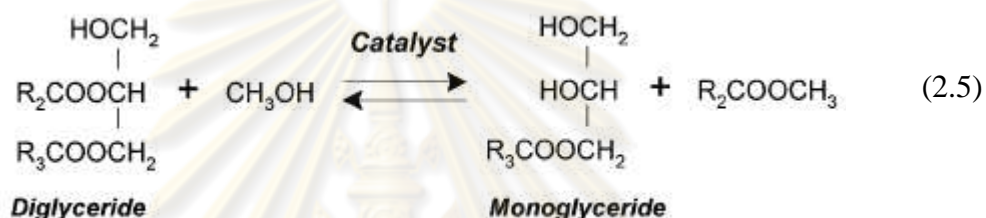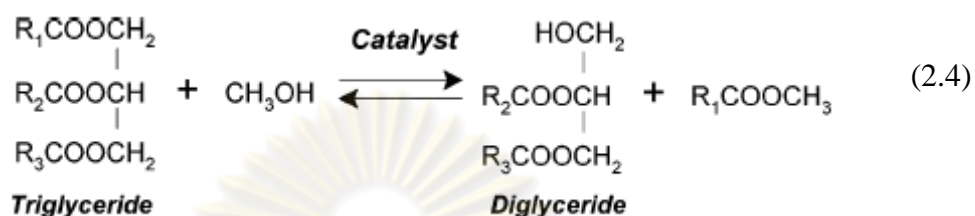
Figure 2.3 Three consecutive transesterifications of triglyceride.

Alcohols used in the transesterification of triglycerides include the primary and secondary monohydric aliphatic alcohols having 1-8 carbon atoms. However, the often used ones are methanol, ethanol, propanol, iso-propanol and butanol. Among these, methanol is the most commonly preferred in the biodiesel production because of its lower cost, high reactivity, and physicochemical properties (polar and shortest chain alcohol). It can easily react with the triglyceride molecules. Moreover, the catalyst can be dissolved in methanol much faster than in other alcohols [36].

2.3.2 Catalytic transesterification

In the transesterification, a catalyst is used to enhance the reaction rate and the alkyl ester yield. Thus, the type and concentration of the catalyst are important, determining the reaction conditions. The catalysts used for the transesterification of triglycerides are classified as acid, base, and enzyme catalysts.

2.3.2.1 Homogeneously base-catalyzed transesterification

Homogeneous base catalyst is an alkaline solution such as sodium hydroxide, sodium methoxide, potassium hydroxide, or potassium methoxide. Currently, the conventional biodiesel production technology is based on NaOH and KOH due to their availability and low cost. The reaction rate in the alkaline process is much faster than others, resulting in much shorter reaction time [1]. The rate of base-catalyzed transesterification was reported as high as 4,000 times faster than that of transesterification in the presence of an acidic catalyst [37].

The mechanism of base-catalyzed transesterification of vegetable oil is shown in Figure 2.4. The first step (Eq.(2.7)) is the reaction of base with alcohol, producing an alkoxide and the protonated catalyst. The alkoxide ion is a strong nucleophile and attacks the carbonyl group of triglyceride, generating a tetrahedral intermediate (Eq.(2.8)), from which the alkyl ester and the corresponding anion of diglyceride are formed (Eq.(2.9)). In the last step, the deprotonation of the catalyst results in the regeneration of active species (Eq. (2.10)). The regenerated catalyst is able to react with the second molecule of alcohol for another catalytic cycle. Diglyceride and monoglyceride are converted by the same mechanism to a mixture of alkyl esters and glycerol [38].

$$ROH + B \rightleftharpoons RO^- + BH^+ \qquad (2.7)$$

$$(2.8)$$

$$(2.9)$$

$$(2.10)$$
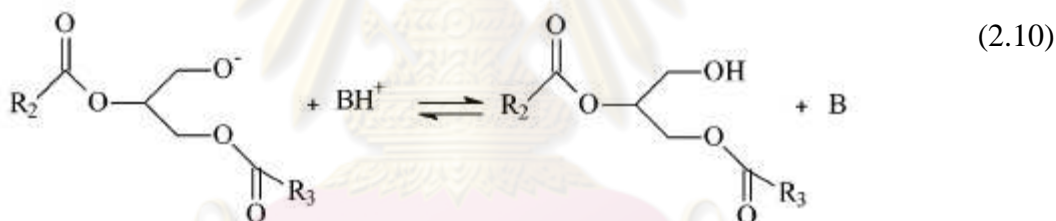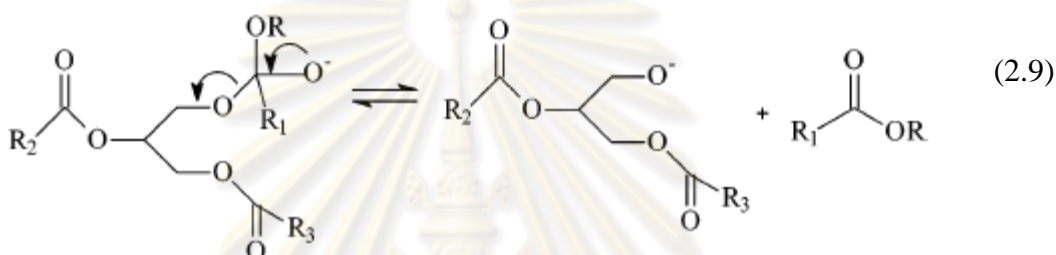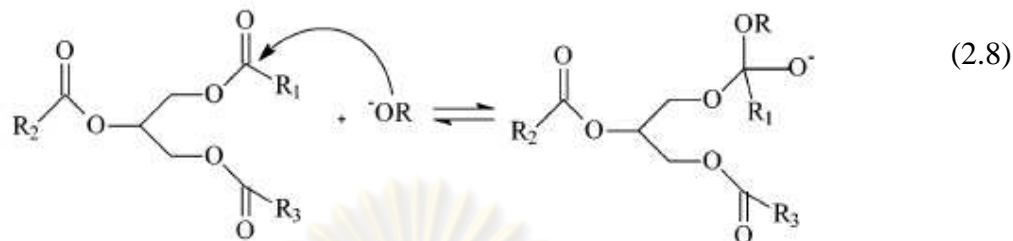
B: base catalyst

R_1, R_2, R_3: carbon chain of the fatty acids

R_4: alkyl group of the alcohol

Figure 2.4 Mechanism of the transesterification of vegetable oils catalyzed by base.

　　　　Even though the transesterification is feasible using homogeneous base catalysts, the base-catalyzed process suffers from many serious problems. The alkaline catalysts should not be used in the transesterification if the feedstock contains free fatty acid with the concentration higher than 0.5 wt.%. Free fatty acid reacts with the alkaline catalyst, resulting in a soap formation (Eq.(2.11). Soap inhibits separation of methyl esters and glycerol, and contributes to emulsion formation during washing. Furthermore, the soap formation increases the viscosity of methyl esters and causes a gel formation.

(2.11)
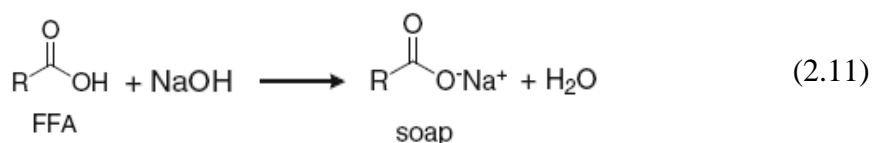
Water promotes the formation of free fatty acids by a hydrolysis of triglyceride as shown in Eq.(2.12). Therefore, the presence of water results in the soap formation as described above.

(2.12)

Triglyceride
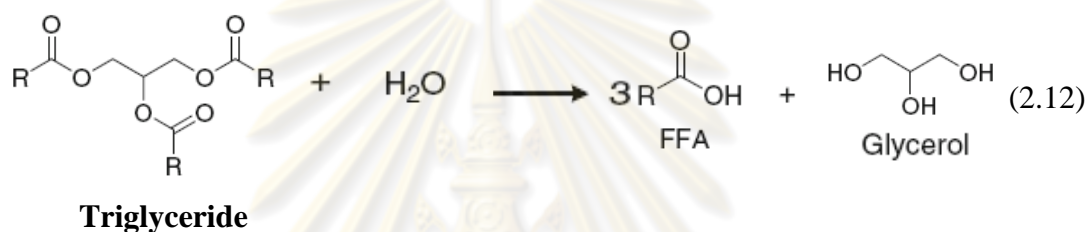
In the presence of residual catalysts, water participates in the hydrolysis of biodiesel to produce additional free fatty acids and methanol as shown in Eq.(2.13).

(2.13)
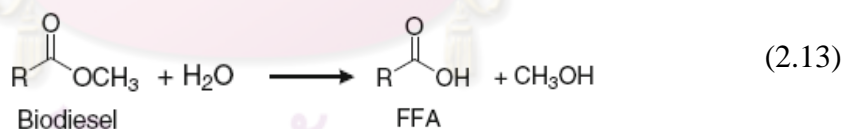
Moreover, water that enhances the soap formation, can be generated by a reaction of sodium hydroxide with methanol during the formation of active species (CH_3O^-) at the initial state of the transesterification reaction (Eq.(2.14)).

$$NaOH + CH_3OH \longrightarrow CH_3\bar{C}Na^+ + H_2O$$

(2.14)
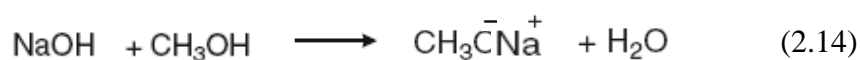
2.3.2.2 Homogeneously acid-catalyzed transesterification

In the transesterification using homogeneous acid catalyst, the reaction can be catalyzed by sulfuric, hydrochloric or sulfonic acids. In general, the acid catalyzed reactions are performed at the high alcohol to oil molar ratios, low to moderate temperatures and pressures, and high acid concentrations to obtain a high product yield. The alcohol to oil molar ratio is one of the main factors influencing the transesterification. However, the excess amount of alcohol makes the recovery of glycerol difficult. Figure 2.5 shows the mechanism of acid-catalyzed transesterification of representative triglyceride. Firstly, the triglyceride carbonyl group is protonated by the acid catalyst (Eq.(2.15)). The activated carbonyl group then undergoes nucleophillic attack from an alcohol molecule, forming a tetrahedral intermediate (Eq.(2.16)). Solvent assisted proton migration give rise to a leaving group, promoting the cleavage of the tetrahedral intermediate and yielding a protonated alkyl monoester and a diglyceride molecule (Eq.(2.17)). The transfer of proton then regenerates the acid catalyst. This sequence is repeated twice to yield 3 alkyl monoesters and glycerol as products [39].

(2.15)

(2.16)

(2.17)
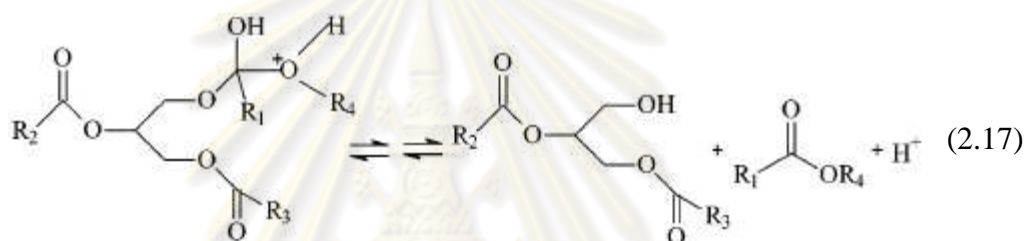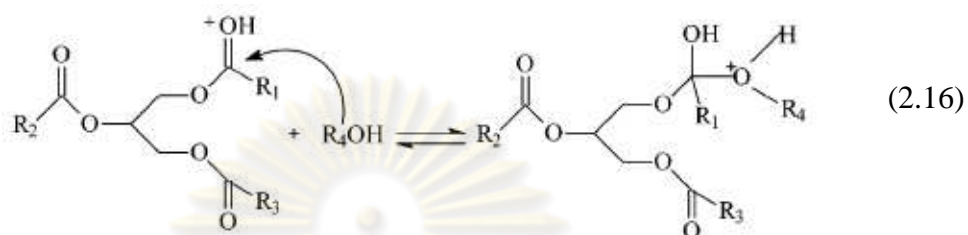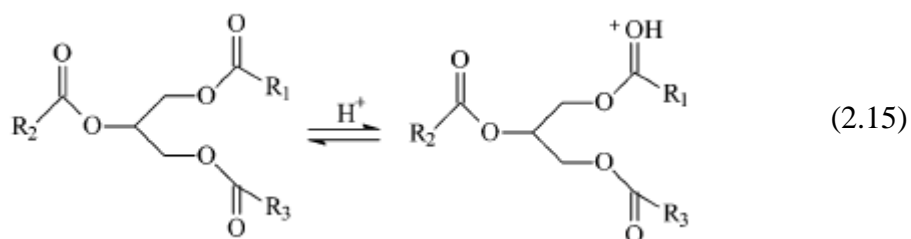
R$_1$, R$_2$, R$_3$: carbon chain of the fatty acids

R$_4$: alkyl group of the alcohol

Figure 2.5 Mechanism of the transesterification of vegetable oils catalyzed by acid.

The acid-catalyzed transesterification holds an important advantage over the base-catalyzed reaction that the performance of the acid catalyst is not strongly influenced by the presence of free fatty acid. Therefore, the acid catalysts can directly produce biodiesel from low-cost feedstocks such as waste cooking oil and greases, associated with a high free fatty acid concentration. However, this process requires more alcohol and larger volume reactors. Besides, the use of acid catalyst requires a special grade stainless steel due to corrosion problem. In some processes, the acid catalysts have been used in conjunction with the base catalysts (two stage reaction process). Typically, an acid catalyst (H_2SO_4, HCl) is initially used to convert free fatty acids to methyl esters (Eq.(2.18)), and then in the second stage, the transesterification of oil is performed in the presence of a base catalyst (NaOH, KOH).

$$HO-\overset{\overset{\displaystyle O}{\|}}{C}-R \ + \ CH_3OH \ \xrightarrow{(H_2SO_4)} \ CH_3-O-\overset{\overset{\displaystyle O}{\|}}{C}-R \ + \ H_2O \qquad (2.18)$$

Fatty acid   Methanol   Methyl ester   Water
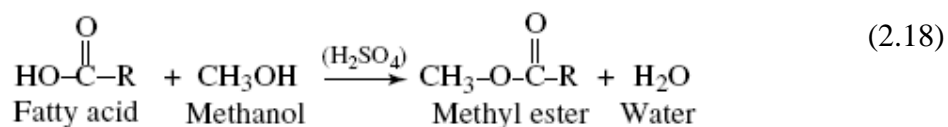
2.3.2.3 Heterogeneously base-catalyzed transesterification

Although the homogeneous catalysis using alkali hydroxides or alkoxides results in the fast reaction rate under mild conditions, there are some drawbacks that originate from the homogeneous catalysts. The removal of these soluble catalysts is difficult and a large amount of alkali wastewater derived from neutralization and washing step is generated. Moreover, the homogeneous base catalysts are sensitive to free fatty acids and water presenting in the feedstocks and alcohols. Free fatty acids react with the hydroxide bases (NaOH, KOH) to form soap. The presence of soap complicates the esters/glycerol separation and decreases the catalytic activity and the yield of fatty acid methyl ester. Water in the feedstock leads to hydrolysis of oils and fatty acid methyl ester. Thus, for the conventional processes using homogeneous catalysts, the free fatty acid and water content in the feedstock must be lower than 0.50, 0.06 wt.%, respectively.

To minimize the problems associated with the use of homogeneous catalysis, heterogeneous catalysts have been extensively investigated and recently introduced to commercial biodiesel production. Heterogeneous catalysts can be easily separated from the reaction mixture and can be reutilized, diminishing waste water found in the conventional process. The cost of biodiesel could be reduced by the use of a heterogeneous catalyst due to simplification of the separation and purification of the products and no loss of methyl ester yield by soap formation. However, the processes using heterogeneous catalysts need higher temperatures to promote the conversion at a reasonable rate. The advantages/disadvantages of homogeneous and heterogeneous catalysis are compared in Table 2.6.

Table 2.6 Comparison of homogeneously and heterogeneously catalyzed transesterification [39]

Factors	Homogeneous catalysis	Heterogeneous catalysis
Reaction rate	Fast and high conversion	Moderate conversion
After treatment	Catalyst cannot be recovered, must be neutralized leading to waste chemical production	Catalyst can be recoverd
Processing methodology	Limited use of continuous methodology	Continuous fixed bed operation possible
Presence of water/ free fatty acids	Sensitive	Less sensitive
Catalyst reuse	Not possible	Possible
Cost	Comparatively costly	Potentially cheaper

Many solid base catalysts have been proposed for biodiesel production. Alkali metal salts supported on alumina were demonstrated as active heterogeneous base catalysts for the transesterification of vegetable oils (Table 2.7). Alumina itself exhibited no activity, but when loading K_2CO_3, KNO_3, KI, KF or KOH and activating at high temperatures, the supported catalysts showed a remarkable enhancement of the triglycerides conversion. K_2O species formed by thermal decomposition of loaded potassium compounds, and the surface Al–O–K groups formed by salt–support interactions were suggested as the active species responsible for the transesterification reaction [4-5].

Table 2.7 Different sodium or potassium supported catalysts used for transesterification of vegetable oils

Catalyst	Oil	Catalyst amount (wt.%)	MeOH/Oil molar ratio	Reaction time (h)	Temperature (°C)	Results
Na/NaOH/Al$_2$O$_3$ [2]	soybean	2	9:1	2	60	conversion = 94%
K$_2$CO$_3$/Al$_2$O$_3$ [3]	triolein	2.5	25:1	1	60	methyl oleate yield = 94%
KNO$_3$/ Al$_2$O$_3$ [4]	soybean	2.5	15:1	7	60	conversion = 87%
KI/Al$_2$O$_3$ [5]	soybean	2.5	15:1	8	65	conversion = 96%
KF/Al$_2$O$_3$ [40]	canola	3	15:1	8	60	biodiesel yield = 99.6%
KOH/Al$_2$O$_3$ [41]	palm	2.5	15:1	2	60	biodiesel yield = 91.1%

However, there are some interests in the leaching of active species on the support. The leaching of potassium on γ- Al$_2$O$_3$ during the reaction was reported, since the oxides of alkali metal group are water-soluble [6]. This result emphasizes the importance of the homogeneous contribution of the leached basic species in the transesterification reaction.

Alkali earth metal oxides are the potential base catalysts for used in transesterification of triglyceride. The origin of basic sites in alkali earth oxides has been generated by the presence of M$^+$ and O^{2-} ion pairs in different co-ordination environments [42]. The basic strength of the group II oxides and hydroxides increased

in the order Mg > Ca > Sr > Ba. Among alkali earth metal oxides, CaO has been widely investigated in the transesterification reaction [7-11] since it possesses high basic strength [10] and low solubility in methanol. MgO which is produced by direct heating of magnesium carbonate or magnesium hydroxide has the weakest basic strength and solubility in methanol among group II oxides. It has been rarely used for biodiesel production. However, the combination of CaO and MgO gave higher alkyl ester yield. The enhancement of alkyl ester formation may occur via a bifunctional catalysis route. ZnO with weakly hydrogenating character also possesses basic properties. It is established that the mixed oxide of Ca and Zn was active in the methanolysis of palm kernel oil [15]. This result emphasizes the advantage of co-existence of two different basic oxide components in the catalyst for transesterification. Therefore, the motivation to use mixed oxides for transesterification is to enhance the basic strength or, to improve the stability of a single metal oxide as in the general approaches of catalyst design. Table 2.8 summarizes different types of single and mixed oxides catalysts used as heterogeneous base catalysts for biodiesel production.

Table 2.8 Different types of single and mixed oxides catalysts used as heterogeneous base catalysts for transesterification of vegetable oils

Catalyst	Oil	Catalyst amount (wt.%)	MeOH/Oil molar ratio	Reaction time (h)	Temperature (°C)	Results
CaO [9]	sunflower	1	13:1	1.5	60	conversion = 94%
CaO [10]	soybean	8	12:1	1.5	65	biodiesel yield = 95%
Ca and Zn mixed oxide [15]	palm kernel	10	30:1	3	60	methyl ester content > 94%

Table 2.8 Different types of single and mixed oxides catalysts used as heterogeneous base catalysts for transesterification of vegetable oils (continued)

Catalyst	Oil	Catalyst amount (wt.%)	MeOH/Oil molar ratio	Reaction time (h)	Temperature (°C)	Results
calcined Mg-Al hydrotalcite [43]	rape	1.5	6:1	4	65	conversion = 90.5%
Mg-La oxides [44]	sunflower	3	20:1	2.2	room temperature	conversion = 100%
MgCa oxides [45]	sunflower	2.5	12:1	1	100	FAME yield = 92%
ZnO-La$_2$O$_3$ [46]	waste oil	2.3	36:1	3	220	biodiesel yield = 92%

2.3.2.4 Heterogeneously acid-catalyzed transesterification

Solid acid catalysts have the strong potential to replace liquid acids, eliminating separation, corrosion and environmental problems. In general, solid acid catalysts used for biodiesel production requires several requirements that govern reactivity. These requirements are presented in the following:

- An interconnected system of large pores
- A moderate to high concentration of strong acid
- A hydrophobic surface

Large interconnected pores would minimize diffusion problems of molecules having alkyl chains, and strong acid sites are needed for the reaction to proceed at acceptable rate. The hydrophobic surface is essential to promote an adsorption of oily hydrophobic species on the catalyst surface and to avoid possible

deactivation of catalytic sites by the strong adsorption of polar byproducts, such as glycerol and water [47]. However, the studies dealing with the use of solid acid catalysts for transesterification are limited due to the low reaction rate and side reactions. As a result, the factors governing the reactivity of solid acid catalysts have not been fully understood. For example, simple correlations between acid strength and activity of the catalyst have not been clearly formulated. Second, the catalyst must have a porous system with interconnecting pores due to diffusional restriction. Although, it is possible to generate these characteristics in the solids, it is not possible to obtain uniform pore architecture with absolute control over the radius or geometry of the pores as well as the stability of the solid in the system.

The studies of transesterification catalyzed by solid acid have been reported in the literature. Most of them are based on zeolites [48], heteropoly acids [49-50], sulfated zirconia [51-52], Nafion resins [53] and organosulfonic funtionalized mesoporous silicas [54]. However, the use of these catalysts to obtain high conversion of triglycerides to biodiesel requires much higher reaction temperatures than base catalysts because of their low activity for transesterification.

2.3.2.5 Enzyme-catalyzed transesterification

In recent years, there has been an interest in the use of enzymes such as lipases for biodiesel production. Lipases (triacylglycerol acylhydrolase, EC 3.1.1.3) are produced by microorganism (fungi and bacteria), animals and plants. Their commercial preparations are derived from microbial sources due to low costs of production and easy modification of properties [55]. There are two major types of enzymatic biocatalyst: (1) extracellular lipases (previously extracted from the living-producing microorganism broth and then purified) and (2) intracellular lipase which still remains either inside or in the cell-producing walls [56]. Both extracellular and intracellular lipases are used for biodiesel synthesis but the majority of research has been conducted by using immobilized extracellular lipases. Various lipases for biodiesel production have been reported. Their examples are lipases from *Candida*

antartica [57-58], *Candida rugasa* [59], *Pseudomonas cepacia* [60], *Pseudomonas fluoresecence* [61], *Rhizomucar miehei* [62] and *Thermomyces lanuginosa* [63].

In general, the enzyme-catalyzed transesterification can be carried out at mild reaction conditions (temperature, 20-50 °C), with the oils from different sources, including waste oils, refined and crude plant oils. Fats containing triglyceride and free fatty acid can be converted to alkyl esters in a one-step process because the lipases catalyze both transesterification and esterification reaction. In addition, the enzymatic process tolerates the water content in the starting oil and increases the biodiesel yield by avoiding soap formation. Another advantage of enzymatic biodiesel production is providing an easy recovery of glycerol without purification or chemical waste production.

On the other hand, the major technical disadvantages of the enzymatic process are its slower reaction rate than the alkaline process and the enzyme inhibition. Poor solubility of methanol in oil and adsorption of glycerol onto the lipase lead to the accumulation of methanol around the enzyme, resulting in the inactivation of the enzyme. The cost of lipase production is the main obstacle for enzymatic biodiesel production in an industrial scale. To lower the cost of the enzymatic process, the immobilization of lipase in suitable support has been developed. Moreover, if the lipase is immobilized, it can be easily separated from the reaction mixture.

2.4 Heterogeneous Catalyst Preparation

Heterogeneous catalysts are frequently defined as solids or mixtures of solids which accelerate chemical reaction without themselves undergoing changes. Generally, the catalysts may be classified according to the preparation procedure as: (i) bulk catalysts or supports and (ii) impregnated catalysts. On this basis the relative preparation methods are: (i) the catalytic active phase is generated as a new solid phase and (ii) the active phase is introduced or fixed on a pre-existing solid by a process which intrinsically depends on the support surface [64].

The catalytic properties of heterogeneous catalysts are strongly affected by the catalyst preparation. The choice of method for preparing a catalyst depends on the physical and chemical characteristics desired in the final composition.

2.4.1 Bulk catalysts and support preparation [65-66]

2.4.1.1 Precipitation

Precipitation is one of the most widely employed preparation methods and may be used to prepare both single component catalysts and supports. Precipitation is usually understood as obtaining a solid from a liquid solution. In the production of precipitated catalysts, the first step is mixing of two or more solutions or suspensions of materials, causing the precipitation of an amorphous or crystalline precipitate or gel. The formation of the precipitate from a homogeneous liquid phase may occur as a result of physical transformations (change of temperature or of solvent, solvent evaporation) but most often is determined by chemical processes (addition of bases or acids, use of complex forming agents).

It is generally desirable to precipitate the desired material in such a form, that the counterions of the precursor salts and the precipitating agent, which can be occluded in the precipitate during the precipitation, can easily be removed by a calcination step. If precipitation is induced by physical means, i.e. cooling or evaporation of solvent to reach supersaturation of the solution, only the counterion of the metal salt is relevant. If precipitation is induced by addition of a precipitating agent, ions introduced into the system via this route also have to be considered. Favorable ions are nitrates, carbonates, or ammonium, which decompose to volatile products during calcination. If the ions do not decompose to volatile products, careful washing of the precipitate is advisable.

The equilibrium between concentrations of particular ions in solution and the solid precipitate is expressed in terms of the solubility product. The solubility product constant, Ksp, is a particular type of equilibrium constant. The equilibrium is formed when an ionic solid dissolves in water to form a saturated solution. The

equilibrium exists between the aqueous ions and the undissolved solid. A saturated solution contains the maximum concentration of ions of the substance that can dissolve at the solution's temperature. Table 2.9 showed the solubility product constant for various compounds.

Table 2.9 Solubility product constant for various compounds [67]

Name	Formula	K_{sp}
Carbonates		
Calcium carbonate	$CaCO_3$	3.4×10^{-9}
Magnesium carbonate	$MgCO_3$	6.8×10^{-6}
Zinc carbonate	$ZnCO_3$	1.6×10^{-10}
Hydroxide		
Calcium hydroxide	$Ca(OH)_2$	5.0×10^{-6}
Magnesium hydroxide	$Mg(OH)_2$	5.6×10^{-12}
Zinc hydroxide	$Zn(OH)_2$	1.2×10^{-17}

The wet solid is converted to the finished catalyst by filtration, washing, drying, forming, calcination and activation. Adjusting production conditions can vary crystallinity, particle size, porosity, and composition of the precipitate or gel.

2.4.1.2 Co-precipitation

In the synthesis of multicomponent systems, the problems are even more complex. Co-precipitation allows one to obtain good macroscopic homogeneity. The term co-precipitation is usually reserved for preparation of multicomponent precipitates, which often are the precursors of binary or multimetallic compound. The composition of the precipitate depends on the differences in solubility between the components and the chemistry occurring during precipitation.

The choice of salts and/or alkali (precursor) depends on availability at a moderate cost, the solubility in the solvent (water), and avoiding an introduction of compounds that can cause negative effects in the final catalyst. Chlorine ions are

known as common poisons and their presence has to be avoided as well as sulfate, which can be reduced to sulfide during the last step of activation. Therefore, nitrate salts or organic compounds, such as formate, oxalate are preferred although some problems can arise with them. However, formate and oxalate compounds are expensive and may not completely decompose during calcination. Nitrate is inexpensive and particularly soluble in water, but calcination has to be controlled because of the exothermic evolution of nitrogen oxides. In the case of the alkali, Na^+, K^+, NH^+_4 hydroxides, carbonates and bicarbonates can be used as precipitating agents.

2.4.2 Supported catalysts preparation [64]

2.4.2.1 Impregnation

Impregnation is the procedure whereby a certain volume of solution containing the metal precursor is contacted with the solid support, then it is aged, usually for a short time, dried and calcined. According to the volume of solution used, two types of impregnation can be distinguished: wet impregnation and incipient wetness impregnation.

In the wet impregnation technique (also called soaking or dipping), an excess of solution is used. After a certain time, the solid is separated from solution, and the excess solvent is removed by drying. The composition of the batch solution will change and the release of debris can form a mud which makes it difficult to completely use the solution.

In incipient wetness impregnation, the volume of the solution of appropriate concentration is equal or slightly less than the pore volume of the support. Control of the operation must be rather precise and repeated applications of the solution may be necessary. The maximum loading is limited by the solubility of precursor in the solution.

2.4.2.2 Ion exchange

Ion exchange consists of replacing an ion in an electrostatic interaction with the surface of a support by another ion species. The support containing ions A is plunged into an excess volume (compared to the pore volume) of a solution containing ions B. Ions B gradually penetrate into the pore space of the support, while ions A pass into the solution, until equilibrium is established corresponding to a given distribution of the two ions between the solid and the solution. For example, using a proper salt solution at ca. 100°C (to increase the exchange rate), it is possible to prepare the acid form of zeolite by exchanging NH_4^+ for Na^+ and successive calcination.

2.4.2.3 Adsorption

Adsorption allows the controlled anchorage of a precursor (in an aqueous solution) on the support. The term adsorption is used to describe all processes where ionic species from aqueous solutions are attracted electrostatically by charged sites on a solid surface. Often consideration is not given to the difference between true ion exchange processes and electrostatic adsorption at the charged surface of oxides. Catalyst systems, which need charge compensating ions are ideal materials for ion exchange (zeolites, cationic clays or layered double hydroxides). Instead most oxide supports, when placed in an aqueous solution, develop a pH-dependent surface charge. These oxides may show a tendency for adsorption of cations ($SiO_2–Al_2O_3$, SiO_2), or anions (ZnO, MgO) or both, cations in basic solutions and anions in acid solutions (TiO_2, Al_2O_3). The surface charge of an oxide depends on its isoelectric point as well as on the pH and ionic strength of the solution.

2.4.2.4 Deposition-precipitation

In deposition–precipitation two processes are involved: (1) precipitation from bulk solutions or from pore fluids; (2) interaction with the support surface. Slurries are formed using powders or particles of the required salt in amounts

sufficient to give the desired loading, then enough alkali solution is added to cause precipitation. However, precipitation in the bulk solution must be avoided, since it gives rise to deposition outside the pores of the support. A well-dispersed and homogeneous active phase is reached when the OH^- groups of the support (for example, the silanols of silica) interact directly with the ions present in the solution, thereby also determining the nature of the phase formed. The nucleation rate must be higher at the surface than in the bulk solution and the homogeneity of the solution must be preserved. A method to obtain uniform precipitation is to use the hydrolysis of urea as a source of OH^- instead of conventional alkali. Urea dissolves in water and decomposes slowly at ca. 90°C., giving a uniform concentration of OH^- in both the bulk and pore solutions. Thus the precipitation occurs evenly over the support surface, making the use of urea the preferred method for amounts higher than 10–20%.

2.5 Literature Survey

In 2004, Kim *et al*. [2] studied the transesterification of soybean oil, using alumina loaded with sodium and sodium hydroxide as a solid base catalyst. They have studied the role of cosolvent in the transesterification process in the presence of solid base catalyst. When n-haxane was added, the immiscible two-phase system was changed to the homogeneous emulsion state. The optimum vegetable oil to n-hexane molar ratio is found to be 5:1. The maximum biodiesel yield of 94% was obtained after optimum conditions were reached using the methanol/oil ratio of 9, the amount of catalyst of 2 wt.%, the reaction time of 2 h, and the temperature of 60°C. The activity of catalyst was closely correlated to the basic sites which determined by temperature programmed desorption of carbon dioxide (TPD-CO_2).The catalyst activity was also compared to NaOH homogeneous catalyst and nearly the same activity was detected.

In 2005, Ebiura *et al*. [3] studied the selective transesterification of triolein with methanol to methyl oleate and glycerol using alumina loaded with alkali metal salts, including K_2CO_3, KF, $LiNO_3$, NaOH, KOH, KNO_3, $NaNO_3$, and $RbNO_3$, as a

solid base catalyst. Among the catalysts, alumina loaded with K_2CO_3 gave methyl oleate and glycerol in the highest yields of 94 and 89%, respectively. The suitable reaction conditions for the transesterification of triolein with methanol over K_2CO_3/Al_2O_3 were the methanol/triolein molar ratio of 25, the reaction time of 1 h, and the temperature of 60°C. Tetrahydrofuran (THF) was used as a solvent. They also compared catalytic activity of K_2CO_3/Al_2O_3 and KOH under the same reaction conditions and found that K_2CO_3/Al_2O_3 showed the same catalytic activity as that of KOH.

In 2006, Xie *et al*. [5] reported the biodiesel production from transesterification of soybean oil using alumina-supported catalysts. The catalysts were prepared by impregnation of potassium compounds, such as KI, KF, and KOH, into alumina to generate catalytic activities for transesterification reaction. The catalyst with 35 wt.% KI loading on Al_2O_3 and calcined at 500°C for 3 h was found to be the optimum catalyst, which gave the highest basicity and the best catalytic activity. The highest conversion of 96% was achieved at reaction condition of a molar ratio of methanol to oil of 15, a reaction time of 8 h, a temperature of 65°C, and a catalyst amount of 2.5 wt.%. It was concluded that there was a correlation between the activities of the catalysts with their corresponding basic properties. The K_2O species formed by thermal decomposition of precursor and the surface Al-O-K groups by precursor-support interaction were revealed as the actives species toward the transesterification.

In 2007, Alonso *et al*. [6] studied the leaching of potassium species from K/γ-Al_2O_3 catalysts in the transesterification of sunflower oil with methanol. A K/γ-Al_2O_3 catalyst was prepared using the wet impregnation method with K_2CO_3 as a precursor salt. They found that this catalyst showed good activity, achieving a methyl ester close to 100% after 1 h. However, when it was used in successive runs the catalyst showed a strong decrease in its catalytic performance, yielding 99% of fatty acid methyl ester in the first run, and only 3.8% for the fourth run. This is due to the leaching of active species. They explained the dissolved active species arise from the

attack of the methanol to the $KAlO_2$-like derived species present at the surface of the alumina.

In 1999, Gryglewicz [7] investigated the possibility of using alkali earth metal hydroxides, oxides, and alkoxides to catalyze the transesterification of rapeseed oil with methanol. He found that NaOH was the most active, $Ba(OH)_2$ was slightly less active, and that $Ca(CH_3O)_2$ showed medium activity. The reaction rate was lowest when CaO was used as catalyst while MgO and $Ca(OH)_2$ showed no catalytic activity. The high activity of barium hydroxide is due to its higher solubility in methanol with respect to other compounds. The order of reactivity $Ca(OH)_2 < CaO < Ca(CH_3O)_2$ agrees with the Lewis theory: the methoxides of alkali earth metals are more basic than their oxides and their hydroxides. The transesterification rate can be increased using ultrasound energy and the cosolvent (THF).

In 2008, Liu *et al*. [10] utilized CaO as a solid base catalyst for transesterification of soybean oil. They revealed that the reaction rate is accelerated in the presence of water, because CaO generated more methoxide anions, which are the real catalyst of transesterification of triglyceride to biodiesel. However, if too much water (more than 2.8% by weight of soybean oil) is added to methanol, the fatty acid methyl ester will hydrolyze under basic conditions to generate fatty acid, which can react with CaO to form soap. Catalyst reusability studies were carried out by activating by methanol with 2.03% water in the first use and reusing them with the analytical reagent methanol in a subsequent reaction cycle. They found that the catalytic activity was maintained even after used for 20 cycles and the biodiesel yield was only slightly decreased. A 12:1 molar ratio of methanol to oil, addition of 8% CaO catalyst, 65°C and 2.03% water content in methanol gave the best results, and the biodiesel yield exceeded 95% at 1.5 h of reaction.

In 2005, Cantrell *et al*. [12] studied the structure-activity correlations of Mg-Al hydrotalcites for transesterification of glyceryl tributyrate with methanol. A series of $[Mg_{(1-x)} Al_x (OH)_2]^{x+}(CO_3)_{x/n}^{2-}$ hydrotalcite materials with composition over the range x = 0.25-0.55 have been synthesized using an alkali-free coprecipitation method. All hydrotalcite materials are effective catalysts for the transesterification of

glyceryl tributyrate with methanol. The rate of glyceryl tributyrate conversion increases steadily with Mg content, and the most active $Mg_{2.93}Al$ catalyst was 10 times more active than MgO. The rate of reaction also correlates with intralayer electron density, which can be associated with increased basicity.

In 2007, Shumaker *et al*. [14] studied the transesterification of soybean oil to fatty acid methyl esters using a calcined Li/Al layered double hydroxide catalyst. The calcination temperature of the catalyst affected on its activity. A temperature of 400-450°C was found to be optimal, corresponding to decomposition of the layered double hydroxide to the mixed oxide without formation of less basic $LiAlO_2$ and $LiAl_5O_8$ phases. It was found that, at the reflux temperature of methanol, the conversion of soybean oil was achieved at low catalyst loadings (2-3 wt.%) and short reaction times (2 h). Catalyst recycling studies showed that the catalyst maintained a high level of activity over several cycles, although analyses indicate that a small amount of Li is leached from the catalyst.

In 2008, Ngamcharussrivichai *et al*. [15] used mixed oxides of Ca and Zn as a solid base catalyst for transesterification of palm kernel oil with methanol. The catalyst was prepared by the co-precipitation of corresponding mixed metal nitrate solution in the presence of Na_2CO_3 as precipitant. The catalyst with a Ca/Zn molar ratio of 2.5 and followed by calcination at 800°C for 2 h exhibited the best catalytic activity for the transesterification. When the transesterification reaction was performed at 60°C, with the methanol/oil molar ratio of 30 and 10 wt.% of catalyst, the methyl ester content reached 94% after 3 h of reaction. They found that washing with the mixture of methanol and 5M NH_4OH is a good method for the regeneration of a spent catalyst. The catalyst can be reused up to 3 times with maintaining the methyl ester content > 90%.

In 2008, Babu *et al*. [44] used magnesium-lanthanum-mixed oxide catalysts in the transesterification of sunflower oil and the catalyst was prepared by a precipitation of nitrate precursors with KOH/K_2CO_3. With increasing Mg content in the mixed oxides, the basicity of the Mg-La oxides increased but the surface area decreased. The

catalyst with a Mg/La weight ratio of 3:1 showed optimum performance toward transesterification of oils, and it exhibited excellent activity even at room temperature. After 2.2 h of reaction time, at room temperature, with 20:1 molar ratio of methanol/oil and 5 wt.% of catalyst content, the maximum conversion achieved was 100%.

In 2008, Albuquerque et al. [45] investigated the transesterification activities of MgAl and MgCa oxides. It was found that MgAl and MgCa oxides were active as basic catalysts for transesterification processes, as evidenced in the reaction between ethyl butyrate and methanol as well as in the methanolysis of sunflower oil. The best performance was observed for the series of MgCa oxides, which could be attributed to the presence of strong basic sites on the surface, mainly associated to Ca^{2+}-O^{2-} pairs, and a surface area much higher than that of pure CaO. The highest activity was found for a Mg:Ca molar ratio of 3.8, with a FAME yield of 92%, for a methanol:oil molar ratio of 12, at a reaction temperature of 333 K and 2.5 wt.% of catalyst were employed.

In 2009, Yan et al. [46] studied the simultaneous transesterification and esterification of unrefined or waste oils over ZnO-La_2O_3 catalysts. A strong interaction between Zn and La species was observed with enhanced catalyst activities. Lanthanum promoted zinc oxide distribution, and increased the surface acid and base sites. The catalyst with 3:1 ratio of zinc to lanthanum was found to simultaneously catalyze the oil transesterification and fatty acid esterification reactions, while minimizing oil and biodiesel hydrolysis. After reaction time of 3 h at 220°C, 96% of fatty acid methyl ester (FAME) was obtained.

In 2008, Tittabut et al. [68] studied the transesterification of glyceryl tributyrate and palm oil with methanol using metal-loaded MgAl oxides. MgAl hydrotalcites (Mg/Al molar ratios 3 and 4) were synthesized using alkali and alkali-free methods at different pH's, followed by the the calcination, and then loaded with Na, K metals at different content. The results suggested that the catalysts synthesized with a Mg/Al molar ratio of 4 and at pH 11 are more basic than those with a ratio of 3

and at pH 8, due to higher incorporation of Mg in the oxides, resulting in higher catalytic activity. For the metal-loaded catalysts, under the same reaction conditions, it was found that the MgAl oxide loaded with 1.5% K gave the highest activity. It was therefore used for the biodiesel synthesis from palm oil. The ester content and yield of biodiesel were 96% and 87% at temperature 100°C in 9 h. The catalyst could be regenerated by recalcination and reloading metal.

In 2009, Chuayplod *et al*. [69] studied the transesterification of rice bran oil with methanol over Mg(Al)La hydrotalcites and Metal/MgAl oxides. Both MgAl and Mg(Al)La hydrotalcites were synthesized by an alkali-free coprecipitation method and calcined to their corresponding oxides. MgAl oxide was impregnated with different kinds of metals (M = Cs, Sr, Ba, and La). The Mg(Al)La oxide obtained from calcination of Mg(Al)La hydrotalcite showed a higher activity than the MgAl oxide. The rehydrated Mg(Al)La hydrotalcite was found to be superior to the calcined one. Biodiesel (97% ester content and 78% product yield) could be produced from rice bran oil by a two-step process: esterification and transesterification reactions catalyzed by the silica-supported $H_3PW_{12}O_{40}$ acid catalyst and the rehydrated Mg(Al)La hydrotalcite, respectively.

In 2009, Albuquerque *et al*. [70] studied the transesterification of ethyl butyrate with methanol using MgO/CaO catalysts. The catalysts were prepared by co-precipitation method in a basic medium and subsequent calcination. Textural properties were improved by the presence of Mg, with the porosity increased and the particle sizes decreased with respect to pure CaO. These catalysts were active in the transesterification of ethyl butyrate with methanol at 333 K and atmospheric pressure, a model reaction to evaluate the potential of these basic catalysts in triglycerides transesterification for biodiesel production. The most active catalyst was obtained with Mg/Ca ratio of 3, with conversion close to 60%.

CHAPTER III

EXPERIMENTAL

3.1 Chemicals

3.1.1 Chemicals for syntheses of catalysts

1. Calcium nitrate ($Ca(NO_3)_2 \cdot 4H_2O$) (AR grade, Ajax Finechem)
2. Magnesium nitrate ($Mg(NO_3)_2 \cdot 6H_2O$) (AR grade, Ajax Finechem)
3. Zinc nitrate ($Zn(NO_3)_2 \cdot 6H_2O$) (AR grade, Ajax Finechem)
4. Sodium carbonate (Na_2CO_3) (AR grade, Ajax Finechem)
5. Nitric acid (HNO_3, 50-70%) (JT. Baker)

3.1.2 Chemicals for transesterification

1. Refined bleach deodorized palm kernel oil (Chumporn Palm Oil Industry Co., Ltd.)
2. Methanol (CH_3OH, 99.5%)
3. Sodium sulfate (Na_2SO_4, 99%) (Riedel-deHaën)

3.1.3 Chemicals for reaction product analysis

1. Methyl undecanoate ($C_{12}H_{24}O_2$, 96%) (ACROS Organics)
2. Heptane (C_7H_{16}) (MERCK)

3.2 Instruments and Equipments

1. Peristaltic pump

2. Beaker, 250, 600 and 1000 mL

3. Magnetic bar

4. Magnetic stirrer

5. Dropper

6. pH meter

7. Water bath

8. Thermometer

9. Suction flask and vacuum pump

10. Filter paper, No. 42

11. Oven

12. Crucible

13. Muffle furnace

14. Desiccator

15. Three-neck round bottom flask, 250 mL

16. Stopper

17. Condensor

18. Thermometer

19. Water bath

20. Magnetic stirrer

21. Magnetic bar

22. Rotary evaporator

23. Centrifuge

3.3 Reaction Product Analysis

The methyl ester (ME) content, equivalent to methyl ester yield, was determined by a Shimadzu GC-14 B gas chromatograph equipped with a 30-m DB-Wax capillary column and a flame ionization detector (FID).

Table 3.1 GC conditions for determination of methyl ester content

Condition	Value
Carrier gas (He) flow rate	1.0 mL/min
Make up gas (He) pressure	100 kPa
Hydrogen pressure (for FID)	60 kPa
Air pressure (for FID)	30 kPa
Detector temperature	250°C
Split ratio	1 : 20
Injection port temperature	250°C
Inject volume	0.5 μL
Initial column temperature	140 °C
Ramp rate	15°C /min
Final column temperature	200°C

Figure 3.1 Gas chromatograph.

3.4 Characterization of Catalysts

3.4.1 Scanning electron microscope [71]

Morphological study of catalysts was carried out with a JEOL JSM-5410 LV Scanning Electron Microscope (SEM). The sample was sputter-coated with gold before the observation. The SEM micrographs were taken by using a 15 kV electron beam with a magnification of 15 - 35,000.
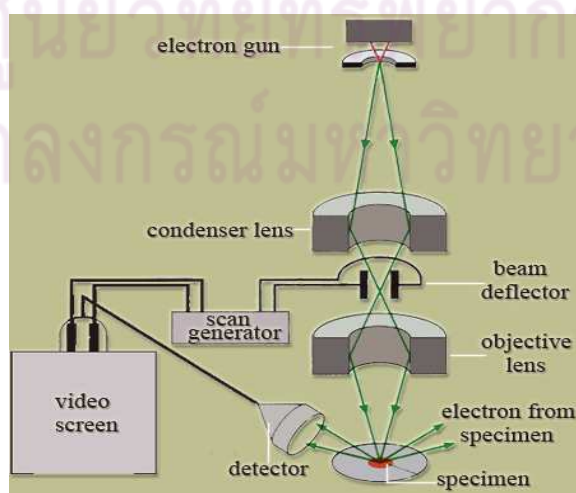
Figure 3.2 Schematic diagram of scanning electron microscope.

Scanning electron microscopy (SEM) involves rastering a narrow electron beam over the surface and detecting the yield of either secondary or backscattered electrons as a function of the position of the primary beam. Contrast is caused by the orientation: Parts of the surface facing the detector appear brighter than parts of the surface with their surface normal, pointing away, from the detector. The secondary electrons have mostly low energies (~5-50 eV) and originate from the surface region of the sample. Backscattered electrons come from deeper and carry information on the composition of the sample, because heavy elements are more efficient scatters and appear brighter in the image.

3.4.2 Surface area and porosity analyzer [72]

The surface area of the calcined catalyst was determined by N_2 adsorption-desorption measurement using a Micromeritics ASAP 2020 surface area and porosity analyzer.

Figure 3.3 Surface area and porosity analyzer

The Brunauer-Emmett-Teller (BET) theory is a rule for the physical adsorption of gas molecules on a solid surface and serves as the basis for an important analysis technique for the measurement of the specific surface area of a material.

The concept of the theory is an extension of the Langmuir theory, which is a theory for monolayer molecular adsorption, to multilayer adsorption with the following hypotheses: (a) gas molecules physically adsorb on a solid in layers infinitely; (b) there is no interaction between each adsorption layer; and (c) the Langmuir theory can be applied to each layer. The resulting BET equation is expressed by (Eq.(3.1)):

$$\frac{1}{v\left[(P_0/P) - 1\right]} = \frac{c-1}{v_m c}\left(\frac{P}{P_0}\right) + \frac{1}{v_m c} \tag{3.1}$$

P and P_0 are the equilibrium and the saturation pressure of adsorbates at the temperature of adsorption, v is the adsorbed gas quantity (for example, in volume units), and v_m is the monolayer adsorbed gas quantity. c is the BET constant, which is expressed by (Eq.(3.2)):

$$c = \exp\left(\frac{E_1 - E_L}{RT}\right) \tag{3.2}$$

E_1 is the heat of adsorption for the first layer, and E_L is that for the second and higher layers and is equal to the heat of liquefaction.

Equation (3.1) is an adsorption isotherm and can be plotted as a straight line with $1 / v[(P_0 / P) - 1]$ on the y-axis and $\varphi = P / P_0$ on the x-axis according to experimental results. This plot is called a BET plot. The linear relationship of this equation is maintained only in the range of $0.05 < P / P_0 < 0.35$. The value of the slope A and the y-intercept I of the line are used to calculate the monolayer adsorbed gas quantity v_m and the BET constant c. The following equations can be used:

$$v_m = \frac{1}{A + I} \tag{3.3}$$

$$c = 1 + \frac{A}{I} \tag{3.4}$$

The BET method is widely used in surface science for the calculation of surface areas of solids by physical adsorption of gas molecules. A total surface area S_{total} and a specific surface area S are evaluated by the following equations:

$$S_{BET,total} = \frac{(v_m N s)}{V} \qquad (3.5)$$

$$S_{BET} = \frac{S_{total}}{a} \qquad (3.6)$$

N: Avogadro's number

s: adsorption cross section

V: molar volume of adsorbent gas

a: molar weight of adsorbed species

3.4.3 X-ray diffractometer

Oxide structure and cluster size of the catalysts were determined by techniques of powder XRD using a Bruker D8 Discover equipped with Cu Kα radiation.

X-ray powder diffractometry is recognized as a powerful technique for the identification of crystalline phases. The technique can also be used for the quantitative analyses of solids.

When an X-ray beam strikes a surface of crystalline sample at an angle θ, a portion of the radiation is scattered by the layer of atoms at the surface. The effect of scattering from the regularly spaced centers of the crystal is a diffraction of the beam. The data of X-ray diffraction indicates that the spacing between layers of atoms and the scattering centers must be spatially distributed in a higher regular way. The diffraction of X-rays by crystal is shown in Figure 3.4.
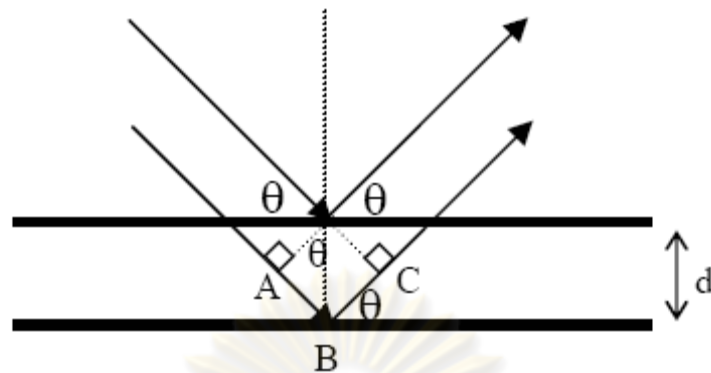
Figure 3.4 Diffraction of X-rays by a crystal.

A narrow beam strikes the crystal surface at angle θ; scattering occurs as a consequence of interaction of the radiation with atoms located at B. The distance was calculated from Equation (3.7).

$$AB \ + \ BC \ = \ n\lambda \tag{3.7}$$

The scattered radiation will be in phase, and the crystal will appear to reflect the X-ray radiation. It is investigated with Eqution (3.8).

$$AB \ = \ BC \ = \ d\sin\theta \tag{3.8}$$

Thus, the condition for constructive interference of the beam at angle θ is expressed by the Equation (3.9), called Bragg's law.

$$2d\sin\theta \ = \ n\lambda \tag{3.9}$$

Where n   =   an integer

d   =   interplanar distance of the crystal (Å; 1 Å= 10^{-10} m)

θ   =   angle between X-ray and crystal planes (degree)

λ   =   wavelength (Å)

3.4.4 X-ray fluorescence spectrometer [73]

Elemental analysis was performed on a Philips PW-2400 ED-2000 Energy Dispersive X-ray Fluorescence Spectrometer (XRF).

An electron can be ejected from its atomic orbital by the absorption of a light wave (photon) of sufficient energy. The energy of the photon must be greater than the energy with which the electron is bound to the nucleus of the atom. When an inner orbital electron is ejected from an atom, an electron from a higher energy level orbital will be transferred to the lower energy level orbital. During this transition a photon maybe emitted from the atom. This fluorescent light is called the characteristic X-ray of the element. The energy of the emitted photon will be equal to the difference in energies between the two orbitals occupied by the electron making the transition. Because the energy difference between two specific orbital shells, in a given element, is always the same (i.e. characteristic of a particular element), the photon emitted when an electron moves between these two levels, will always have the same energy. Therefore, by determining the energy (wavelength) of the X-ray light (photon) emitted by a particular element, it is possible to determine the identity of that element.

For a particular energy (wavelength) of fluorescent light emitted by an element, the number of photons per unit time (generally referred to as peak intensity or count rate) is related to the amount of that analyte in the sample. The counting rates for all detectable elements within a sample are usually calculated by counting, for a set amount of time, the number of photons that are detected for the various analytes' characteristic X-ray energy lines. It is important to note that these fluorescent lines are actually observed as peaks with a semi-Gaussian distribution because of the imperfect resolution of modern detector technology. Therefore, by determining the energy of the X-ray peaks in a sample's spectrum, and by calculating the count rate of the various elemental peaks, it is possible to qualitatively establish the elemental composition of the samples and to quantitatively measure the concentration of these elements.
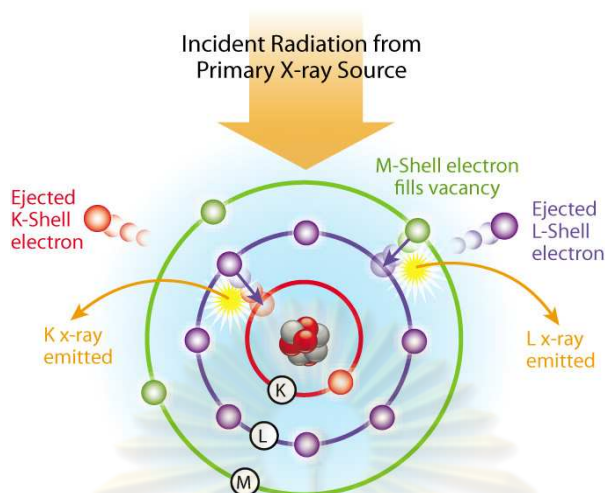
Figure 3.5 Schematic of the XRF process.Incident x-ray knocks out an inner shell electron, higher shell electron fills the empty vacancy and excess energy given up as an x-ray (photon).

3.4.5 Thermogravimetric/differential thermal analyzer [74-75]

Thermogravimetric analysis (TGA) was carried out by using a Perkin Elmer Pyris Diamond thermogravimetric/differential thermal analyzer. Typically, 10 mg of a sample was placed in a platinum pan and heated from 40 to 1,000°C at a ramping rate of 8°C /min with air flow rate of 50 mL/min.

Figure 3.6 Thermogravimetric/Differential Thermal Analyzer.

Thermogravimetric Analysis or TGA is a type of testing that is performed on samples to determine changes in weight in relation to change in temperature. Such analysis relies on a high degree of precision in three measurements: weight, temperature, and temperature change. As many weight loss curves look similar, the weight loss curve may require transformation before results may be interpreted. A derivative weight loss curve can be used to tell the point at which weight loss is most apparent. Again, interpretation is limited without further modifications and deconvolution of the overlapping peaks may be required.

TGA is commonly employed in research and testing to determine characteristics of materials such as polymers, to determine degradation temperatures, absorbed moisture content of materials, the level of inorganic and organic components in materials, decomposition points of explosives, and solvent residues. It is also often used to estimate the corrosion kinetics in high temperature oxidation.

Differential thermal analysis (or DTA) is a thermoanalytic technique, similar to differential scanning calorimetry. In DTA, the material under study and an inert reference are made to undergo identical thermal cycles, while recording any temperature difference between sample and reference. This differential temperature is then plotted against time, or against temperature (DTA curve). Changes in the sample, either exothermic or endothermic, can be detected relative to the inert reference. Thus, a DTA curve provides data on the transformations that have occurred, such as glass transitions, crystallization, melting and sublimation. The area under a DTA peak is the enthalpy change and is not affected by the heat capacity of the sample.

3.4.6 Chemisorption analyzer [76]

The basic properties of the catalysts were investigated by the temperature-programmed desorption (TPD) method, using CO_2 as probe molecule, using a Micromeritics AutoChem II 2920.

Figure 3.7 Chemisorption analyzer.

The interaction of reactants with the catalyst surface is a key parameter in heterogeneous reaction systems. For example, the temperature at which species are desorbed from a surface is indicative of the strength of the surface bond: the higher the temperature, the stronger the bond. Therefore the adsorption of a probe molecule at low temperature, and subsequent monitoring of its desorption/reaction characteristics with temperature, is a simple way to characterize surface properties of catalysts and adsorbents. This is the basis of temperature-programmed analysis methods in which, for a linear increase in temperature, the concentration of the reacting/desorbing particles is recorded as a function of temperature.

Temperature-programmed desorption (TPD) of carbon dioxide is frequently used to measure the number and strength of basic sites. The strength and amount of basic sites are reflected in the desorption temperature and the peak area, respectively, in a TPD plot. However, it is difficult to express the strength in a definite scale and to count the number of sites quantitatively. Relative strengths and relative numbers of basic sites on the different catalysts can be estimated by carrying out the TPD experiments under the same conditions. If the TPD plot gives a sharp peak, the heat of adsorption can be estimated.

3.5 Catalyst Preparation

A mixed oxide of Ca, Mg and Zn was prepared by pH-controlling co-precipitation method. A required quantity of $Ca(NO_3)_2 \cdot 4H_2O$, $Mg(NO_3)_2 \cdot 6H_2O$ and $Zn(NO_3)_2 \cdot 6H_2O$ was dissolved in deionized water. The mixed metal solution was precipitated by adding an aqueous solution of Na_2CO_3 under vigorous stirring. The pH of the resulting solution was varied by adding HNO_3 solution. The amount of CO_3^{2-} was controlled according to two different conditions.

Table 3.2 The catalyst preparation conditions used in the preparation of CaMgZn mixed oxides

Condition	CO_3^{2-}/metal ion molar ratio	Na_2CO_3 concentration (M)
I	1	0.75
II	1.5	1.5

The precipitate was further aged at room temperature or 60°C for 8-20 h. Finally, the white solid was filtered, washed with deionized water, dried in an oven at 100°C overnight, and calcined in a muffle furnace at 800°C for 2 h. Hereafter, the mixed oxide catalysts were designated as CaMgZnXXX-Y, where XXX and Y represent the atomic ratio of Ca:Mg:Zn in the synthesis mixture and the preparation conditions I or II, respectively.

3.6 Transesterification of Palm Kernel Oil with Methanol

A 250-mL three-neck round bottom flask equipped with a condenser and a magnetic stirrer was used as a reactor for transesterification of palm kernel oil. In a typical reaction, 0.6 g of a calcined catalyst was suspended in methanol. Temperature of the mixture was controlled at 60°C by using a water bath. Then, palm kernel oil was added into the mixture under vigorous stirring. In the study of effects of reaction conditions, the various reaction conditions such as catalyst amount (2-6 wt.%), molar ratio of methanol to oil (9:1-20:1) and reaction time (0.5-4 h) were investigated. After

the course of reaction (3 h), the catalyst was separated from the reaction mixture by centrifugation and the excess methanol was removed by using a rotary evaporation. Methyl ester layer was subsequently washed with deionized water and dried with Na_2SO_4. The methyl ester (ME) content, equivalent to methyl ester yield, was determined by a gas chromatograph (GC) equipped with a 30-m DB-Wax capillary column and a flame ionization detector (FID). Methyl ester (ME) content was calculated based on the standard method EN14103 using methyl undecanoate (C_{11}) as the reference standard.

CHAPTER IV

RESULTS AND DISCUSSION

4.1 Catalysts Characterization

4.1.1 Effects of metal composition

The effects of metal composition on the physicochemical properties of catalysts were studied. The catalysts were prepared according to the condition I; the molar ratio of CO_3^{2-}/metal ion of 1, the CO_3^{2-} concentration of 0.75 M, the aging temperature of 60°C, and the aging time of 20 h.

The elemental compositions of mixed oxides synthesized with different amounts of metal precursor are presented in Table 4.1. The Ca:Mg:Zn molar ratios found in the precipitated mixed oxides in all cases were deviated from those in the synthesis mixtures. It should be mainly attributed to the fact that Ca^{2+} and Mg^{2+} are precipitated at pH higher than the pH of synthesis mixture, while Zn^{2+} is readily precipitated at pH of 4 [15]. Therefore, the amount of Zn found in the resulting solid was highest. Although the amount of Mg in the synthesis mixture was increased to the ratio of 1:3:1, the solid with the Ca:Mg:Zn ratio of 1:1:1 was attained, suggesting the low precipitation of Mg^{2+}.

Table 4.1 Elemental composition of calcined CaMgZn catalysts prepared with different Ca:Mg:Zn molar ratios

Catalyst	Ca:Mg:Zn molar ratio[a]		Metal composition in the solid (wt.%)		
	Mixture[b]	Solid[c]	CaO	MgO	ZnO
MgZn11-I	0:1:1	0:1:4	0.0	10.7	89.2
CaMgZn111-I	1:1:1	6:1:7	37.9	4.0	58.0
CaMgZn311-I	3:1:1	19:1:7	63.1	2.3	34.6
CaMgZn131-I	1:3:1	1:1:1	29.8	20.4	49.6
CaMgZn113-I	1:1:3	1:1:4	17.9	9.6	72.3

[a] Determined by XRF spectroscopy.

[b] Ca:Mg:Zn molar ratio in the synthesis mixture.

[c] Ca:Mg:Zn molar ratio in the final solid.

Figure 4.1 shows the XRD patterns obtained from calcined CaMgZn precipitates with different Ca:Mg:Zn molar ratios. In the XRD pattern of MgZn11-I, the presence of MgO and ZnO phases was observed (Figure 4.1a). The calcined CaMgZn showed the diffraction peaks related to CaO, MgO and ZnO phases (Figure 4.2b-4.2e). By varying the metal composition, the diffraction peaks associated with the corresponding metal oxide species became more intense. For an exmple, the peak of MgO observed for CaMgZn131-I possessed higher intensity than those found in MgZn11-I, CaMgZn111-I, CaMgZn113-I, and CaMgZn311-I. Moreover, the diffraction peaks of $Ca(OH)_2$ were observed for all CaMgZn catalysts, suggesting hydration of CaO by moisture in the atmosphere.
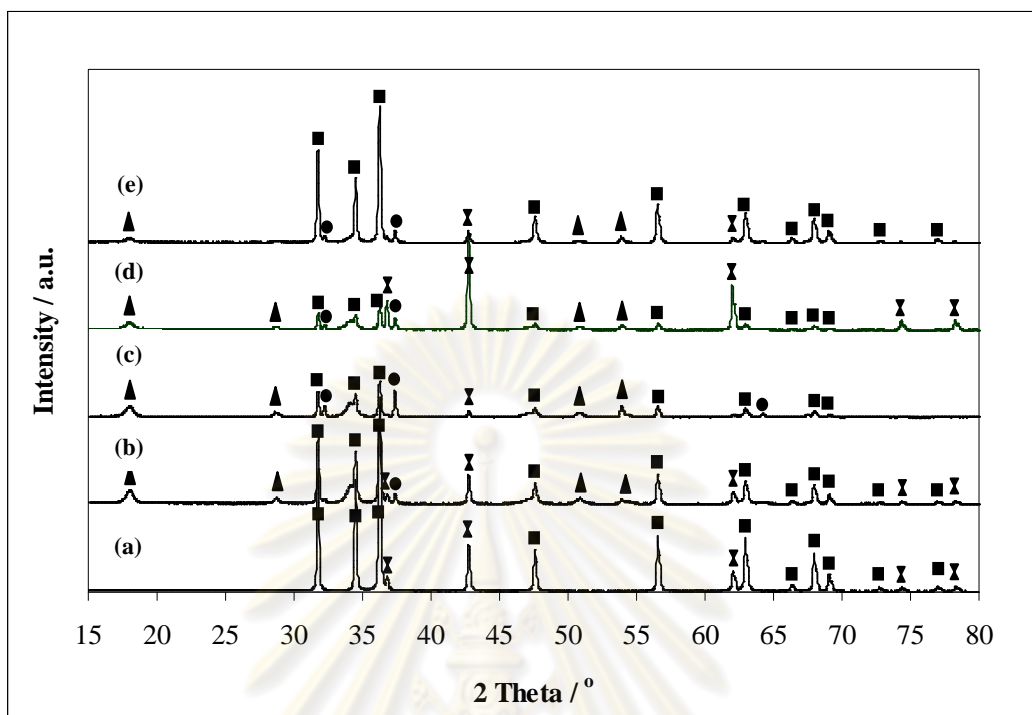
Figure 4.1 XRD patterns of CaMgZn precipitates prepared with different Ca:Mg:Zn molar ratios after the calcination at 800°C: (a) MgZn11-I, (b) CaMgZn111-I, (c) CaMgZn311-I, (d) CaMgZn131-I, and (e) CaMgZn113-I. (Symbols: (●) CaO, (▲) Ca(OH)$_2$, (✗) MgO and (■) ZnO)

During the preparation of CaMgZn catalyst, CaO, MgO and ZnO generated after the calcination of CaMgZn precipitate. Non-calcined MgZn11 showed a major weight loss from 240 to 370°C with a maximum DTG peak at 318°C (Figure 4.2). This process corresponds to the decomposition of basic Zn carbonate $Zn_3CO_3(OH)_4.2H_2O$ reported by Sawada et al. [77]. The decomposition pattern of non-calcined CaMgZn111-I (Figure 4.3) exhibited a three-step weight loss. The first and second peak should correspond to $Zn_3CO_3(OH)_4.2H_2O$ and $Ca(OH)_2$, respectively. The peak at the highest temperature (710°C) should be $CaCO_3$. The TGA results obtained from non-calcined CaMgZn311-I (Figure 4.4) showed a similar decomposition pattern to CaMgZn111-I. It can be seen that the peak corresponding to $CaCO_3$ decomposition was shifted to higher temperature with increasing the amount of Ca. In the case of non-calcined CaMgZn131-I (Figure 4.5), the peak at around

400°C can be assigned to the decomposition of $MgCO_3$. The higher-temperature peaks can be assigned to the $Ca(OH)_2$ and $CaCO_3$ decomposition, respectively. The presence of $ZnCO_3$ and $CaCO_3$ phase in non-calcined CaMgZn113-I was revealed by the DTG peak at 245-300°C and 625-690°C, respectively (Figure 4.6).
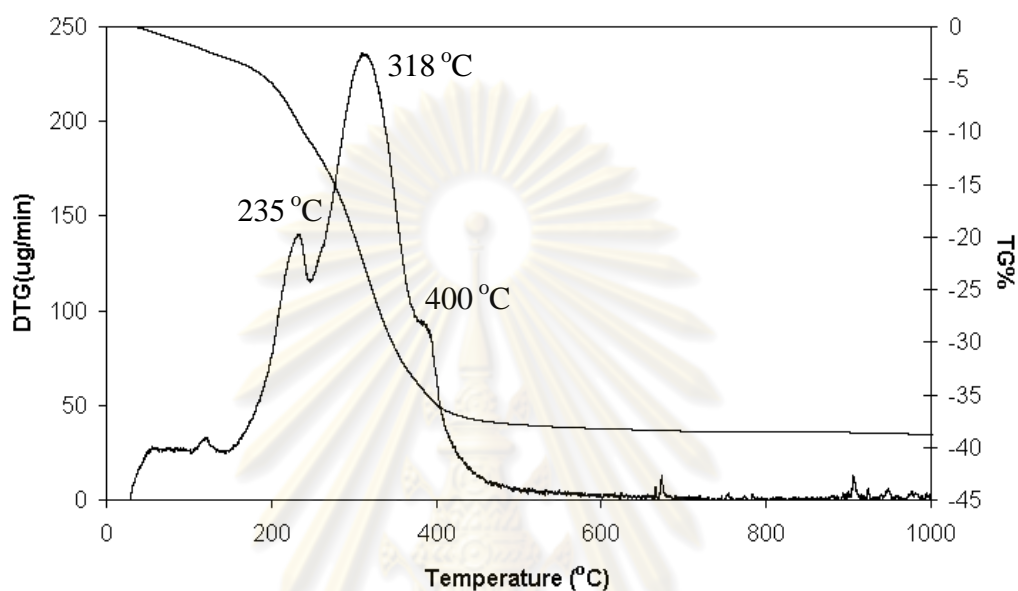
Figure 4.2 Weight loss and differential weight loss (DTG) curves of as-synthesized MgZn11-I.
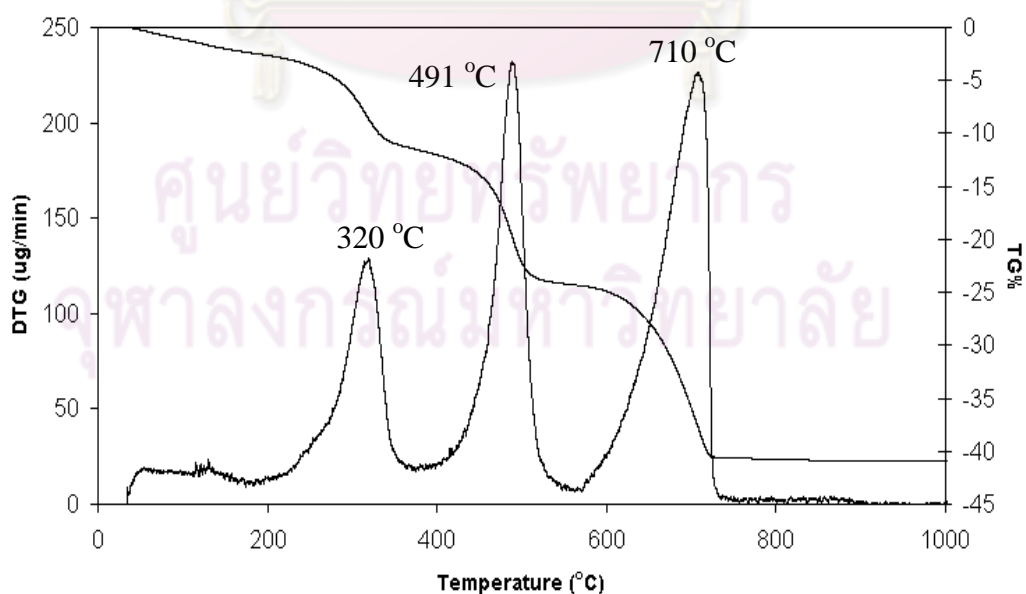
Figure 4.3 Weight loss and differential weight loss (DTG) curves of as-synthesized CaMgZn111-I.
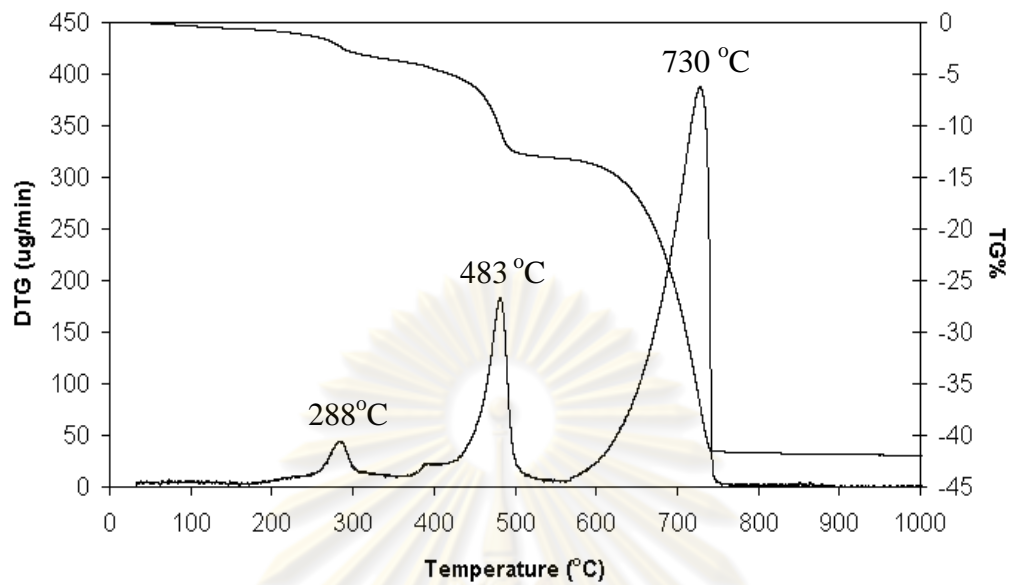
Figure 4.4 Weight loss and differential weight loss (DTG) curves of as-synthesized CaMgZn311-I.
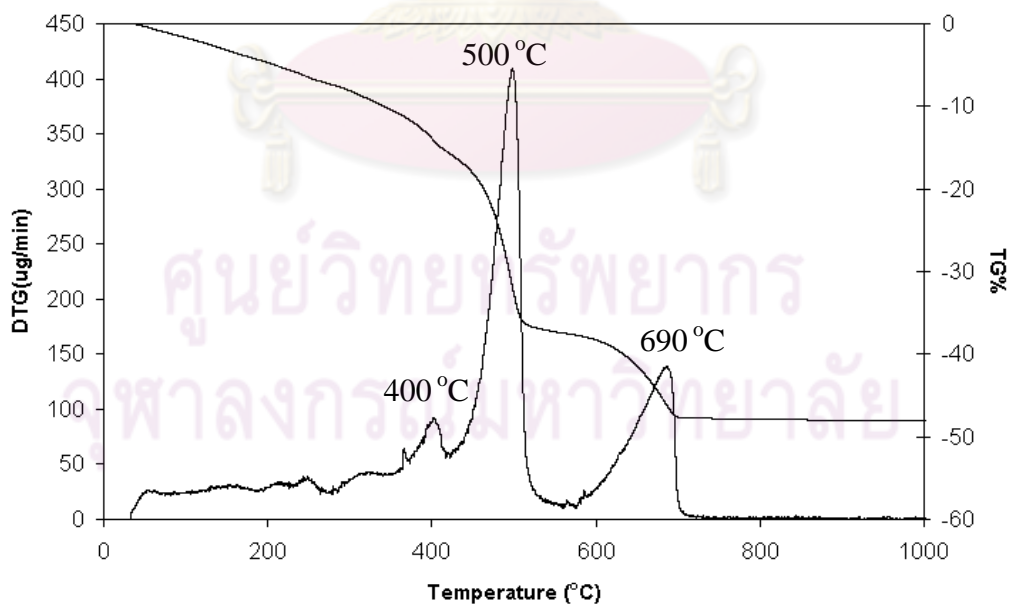
Figure 4.5 Weight loss and differential weight loss (DTG) curves of as-synthesized CaMgZn131-I.
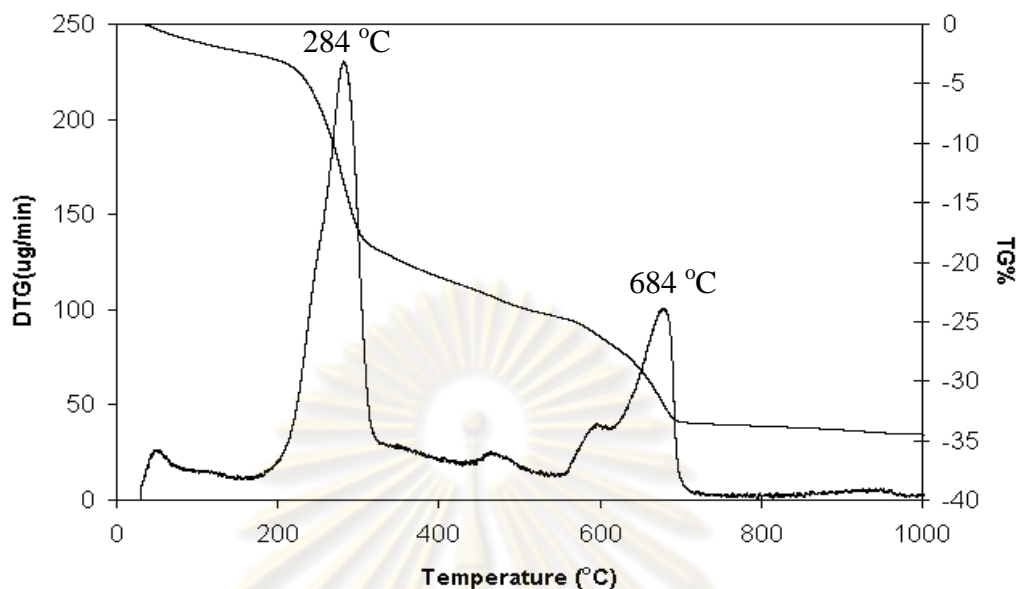
Figure 4.6 Weight loss and differential weight loss (DTG) curves of as-synthesized CaMgZn113-I.

The SEM images of as-synthesized CaMgZn precipitates with different Ca:Mg:Zn molar ratios are shown in Figure 4.7. MgZn11-I showed an aggregate of very small thin flake particles (Figure 4.7a). In the presence of Ca, the formation of spherical particles with various sizes was observed (Figure 4.7b-4.7d). The mixed precipitate particles of CaMgZn111-I possessed non-uniform size and morphology (Figure 4.7b). The presence of both flakes and spheres with a wide range of size distribution can be seen. The increase in the Ca content, CaMgZn311-I (Figure 4.7c), uniformly reduced the particle sizes to 2-3 μm. Similarly, compared to CaMgZn111-I (Figure 4.7b), CaMgZn131-I with increasing amount of Mg exhibited much smaller particle sizes (ca. 1 μm) (Figure 4.7d). On the other hand, the morphology of CaMgZn113-I (Figure 4.7e-4.7f) was an aggregate of flake-like particles similarly to that of MgZn11-I (Figure 4.7a). However, the incorporation of Ca distorted of the particle shape to shortened and thick pellets (Figure 4.7f).
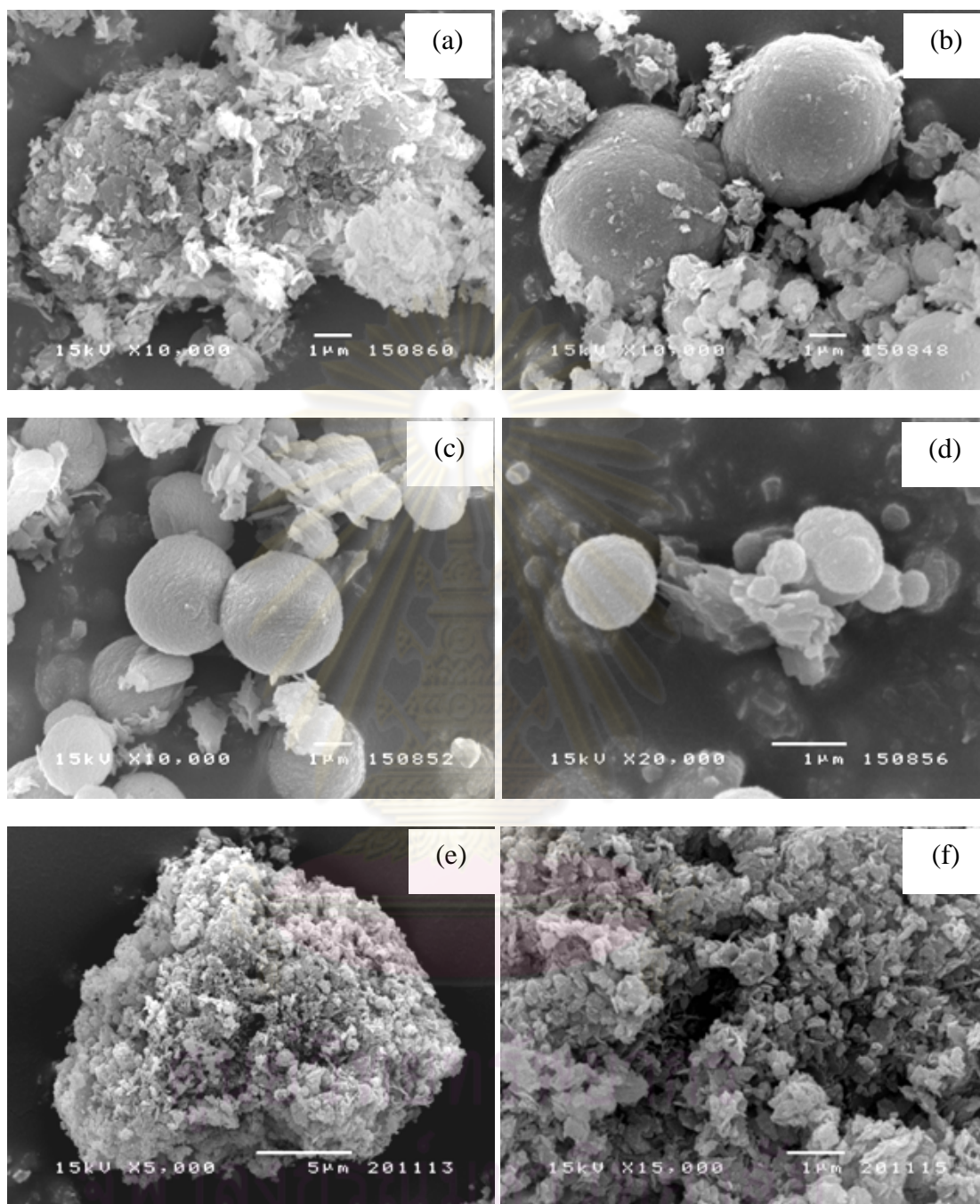
Figure 4.7 SEM images of as-synthesized CaMgZn precipitates prepared with different Ca:Mg:Zn molar ratios: (a) MgZn11-I, (b) CaMgZn111-I, (c) CaMgZn311-I, (d) CaMgZn131-I, (e) CaMgZn113-I and (f) CaMgZn113-I (x15,000).

The textural properties of CaMgZn mixed oxides were characterized by N_2 adsorption desorption measurement and the results are given in Table 4.2. The BET surface area of CaMgZn mixed oxides varied between 2 and 5 m^2g^{-1}.

The cluster sizes of CaO, MgO, and ZnO were calculated by Deby-Scherrer equation. The cluster size of the corresponding metal oxide was increased with increasing the metal content. For example, the cluster size of CaO increased from 47.9 to 49.4 nm as the Ca content in the CaMgZn oxides increased.

Table 4.2 Textural properties of calcined CaMgZn catalysts prepared with different Ca:Mg:Zn molar ratios

Catalyst	Particle size[a] (μm)	Cluster size[b] (nm)			S_{BET}[c] ($m^2 g^{-1}$)	V_{ave}[d] ($mm^3 g^{-1}$)	D_{ave}[e] (Å)
		CaO	MgO	ZnO			
MgZn11-I	0.3-0.5	-	37.9	46.4	5.0	9.9	78.8
CaMgZn111-I	4.0-5.0	47.9	35.6	40.8	3.7	6.8	73.8
CaMgZn311-I	2.0-3.0	49.4	41.6	41.7	1.8	3.8	84.8
CaMgZn131-I	1.0-2.0	42.0	40.6	41.8	4.3	8.6	79.4
CaMgZn113-I	0.2-0.3	43.0	37.9	42.8	4.6	7.4	63.2

[a] Determined by SEM technique.

[b] Determined from XRD patterns using Sherrer's equation.

[c] BET surface area.

[d] Average pore volume.

[e] Average pore diameter.

The CO$_2$ desorption profiles from the temperature-programmed desorption (TPD) analysis are shown in Figure 4.8. A broad peak of MgZn11-I (Figure 4.8a) was observed between 100 and 320°C, which can be attributed to CO$_2$ desorbed from the basic ZnO. Pure calcium oxide derived from CaCO$_3$ showed a desorption peak at 660 °C (Figure 4.8b). CaMgZn111-I and CaMgZn131-I exhibited a similar desorption profile (Figure 4.8c and 4.8e, respectively). The peaks located at 630 °C were ascribed to the desorption of CO$_2$ from the basic CaO sites. Moreover, it was found that the desorption peak slightly shifted to the lower temperatures when compared to pure CaO. CaMgZn311-I (Figure 4.8d) possessed two desorption peaks, which indicated the presence of at least two types of basic sites with different strengths. It should be related to the high Ca content. CaMgZn113-I showed the peak related to CO$_2$ desorbed from CaO at 632°C, while the desorption peak appearing at 190°C corresponded to ZnO (Figure 4.8f).
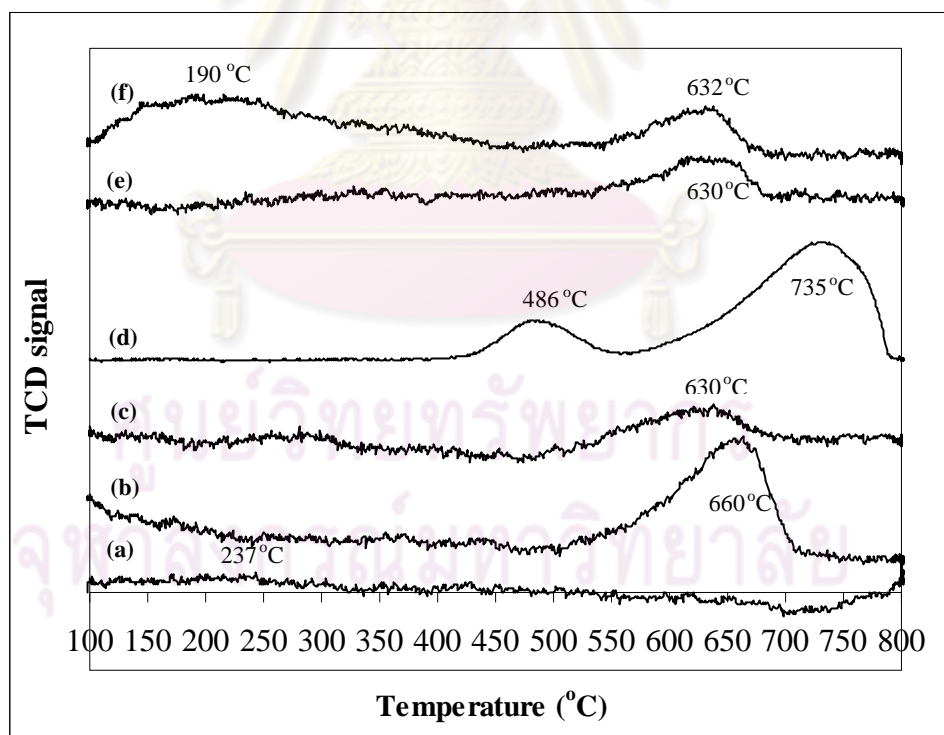
Figure 4.8 CO$_2$-TPD analysis of calcined CaMgZn catalyst prepared with different Ca:Mg:Zn molar ratios: (a) MgZn11-I , (b) CaO (from CaCO$_3$), (c) CaMgZn111-I, (d) CaMgZn311-I, (e) CaMgZn 131-I, and (f) CaMgZn113-I.

4.1.2 Effects of molar ratio of CO_3^{2-}/metal ion

The elemental compositions of mixed oxides synthesized with different molar ratios of CO_3^{2-}/metal ion are summarized in Table 4.3. The molar ratio of CO_3^{2-}/metal ion varied from 0.75 to 1.5. The Ca:Mg:Zn molar ratio and the CO_3^{2-} concentration were kept constant at 1:1:1 and 0.5 M, respectively. The Ca:Mg:Zn molar ratios found in the precipitated mixed oxides were deviated from those in the synthesis mixtures. It should be due to the fact that each metal ion precipitating at different pH as mentioned above.

Table 4.3 shows the influences of the CO_3^{2-}/metal ion molar ratio on the elemental composition of mixed oxides. The amount of MgO in the mixed oxides increased when the molar ratio of CO_3^{2-}/metal ion increased from 0.75 to 1.5. This result suggested that the precipitation of Mg^{2+} at pH of 7 required the high amount of CO_3^{2-}.

Table 4.3 Elemental composition of calcined CaMgZn prepared with different molar ratios of CO_3^{2-}/metal ion

Catalyst	CO_3^{2-} /metal ion	$[CO_3^{2-}]$ (M)	Ca:Mg:Zn molar ratio[a]		Metal composition in the solid (wt.%)		
			Mixture[b]	Solid[c]	CaO	MgO	ZnO
CaMgZn111	0.75	0.5	1:1:1	8:1:9	36.2	3.2	60.2
	1.0	0.5	1:1:1	9:1:9	38.2	3.2	58.5
	1.5	0.5	1:1:1	3:1:4	30.8	7.6	61.4

[a] Determined by XRF spectroscopy.

[b] Ca:Mg:Zn molar ratio in the synthesis mixture.

[c] Ca:Mg:Zn molar ratio in the final solid.

The dependence of morphology of CaMgZn precipitates on the molar ratios of CO_3^{2-}/metal ion is shown in Figure 4.9. There were two types of morphologies. The spherical particles possessed the diameters of 4-5 µm and the other type was flake-like particles. The formation of thin flakes was related to the presence of MgZn mixed precipitates. At the high CO_3^{2-}/metal ion molar ratio, the Mg^{2+} was more precipitated, leading to the increased amount of MgZn phase.
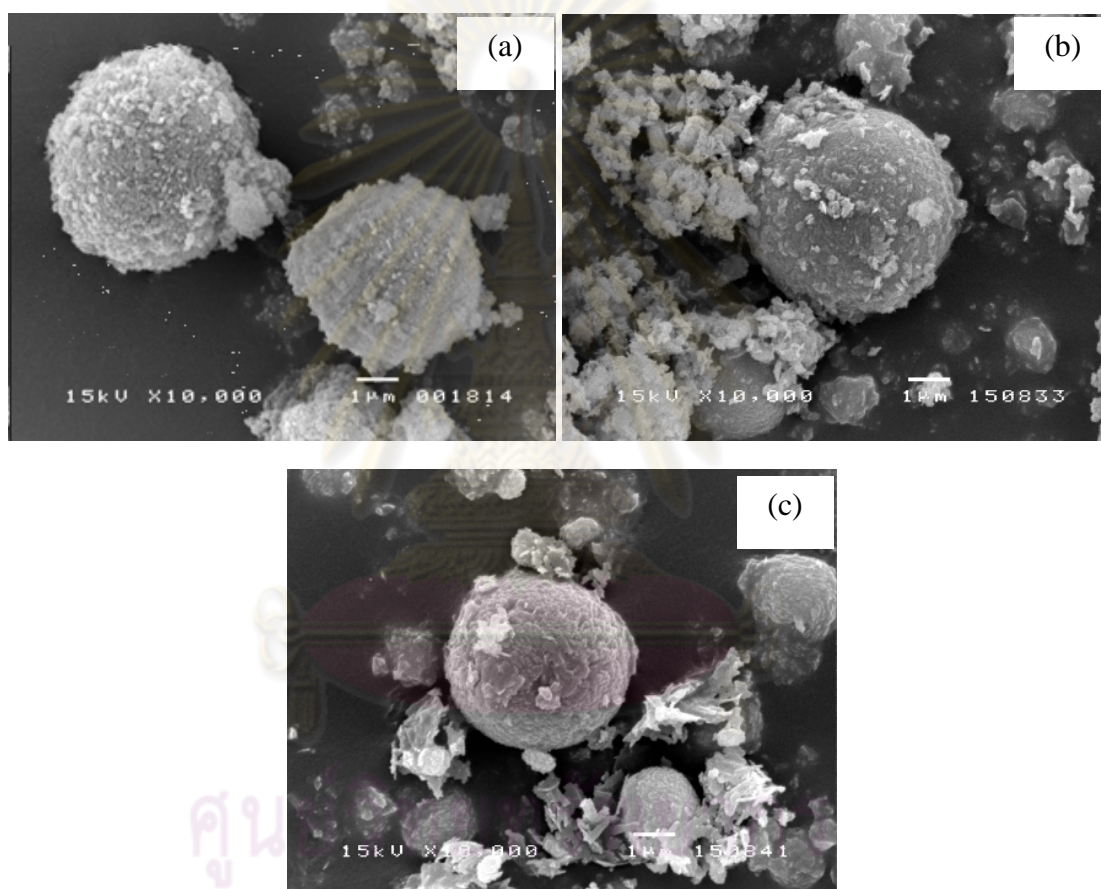
Figure 4.9 SEM images of as-synthesized CaMgZn precipitates prepared with different CO_3^{2-}/metal ion molar ratios: (a) 0.75, (b) 1, and (c) 1.5.

4.1.3 Effects CO_3^{2-} concentration

The influences of CO_3^{2-} concentration on the elemental composition of CaMgZn mixed oxides were studied. The CO_3^{2-} concentration were varied investigated at 0.5, and 1.0 M. Table 4.4 shows that MgO was attained at the highest amount when the mixed oxide prepared with the CO_3^{2-} concentration of 1.0 M, indicating that Mg^{2+} was more precipitated. In addition, the Ca:Mg:Zn molar ratio was very close to 1:1:1 when the CO_3^{2-} concentration of 1.0 M was used as the precipitant.

Table 4.4 Elemental composition of calcined CaMgZn prepared with different CO_3^{2-} concentrations

Catalyst	CO_3^{2-} /metal ion	$[CO_3^{2-}]$ (M)	Ca:Mg:Zn molar ratio[a]		Metal composition in the solid (wt%)		
			Mixture[b]	Solid[c]	CaO	MgO	ZnO
CaMgZn111	1.5	0.5	1:1:1	3:1:4	30.8	7.6	61.4
	1.5	1.0	1:1:1	1:1:1	32.9	17.7	49.3

[a] Determined by XRF spectroscopy.

[b] Ca:Mg:Zn molar ratio in the synthesis mixture.

[c] Ca:Mg:Zn molar ratio in the final solid.

Figure 4.10 shows the influences of CO_3^{2-} concentration on the morphology of the CaMgZn precipitates. As the CO_3^{2-} concentration increased, the precipitate amount was increased. Thus high concentration of CO_3^{2-} did not only enhance the formation of thin flakes related to MgZn phase, but also resulted in the aggregation of the flakes to more uniform spherical particles.
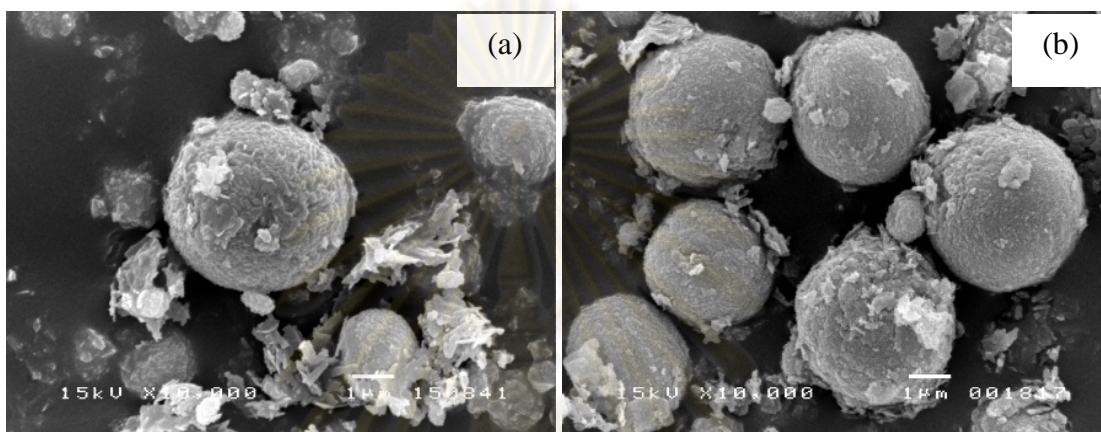
Figure 4.10 SEM images of as-synthesized CaMgZn precipitates prepared with different CO_3^{2-} concentration: (a) 0.5 M. and (b) 1.0 M.

4.1.4 Effects of pH during precipitation

The influences of pH during the precipitation on the structure of the as-synthesized CaMgZn precipitates were investigated by XRD. Figure 4.11 showed the XRD patterns of the as-sythesized CaMgZn precipitates prepared at pH of 7, 8, 9 and 10. These as-synthesized catalysts exhibited similar patterns. They showed the diffraction peaks related to $CaZn(CO_3)_2$, $CaMg(CO_3)_2$, $Zn(OH)_2$ and $Mg(OH)_2$ phases. By consulting the XRF data, the absence of $Mg(OH)_2$ for the as-sythesized precipitate prepared at pH of 7 (Figure 4.11a), suggested the remaining of Mg^{2+} in the aqueous phase. The formation of $Mg(OH)_2$ phase at pH > 7 implied that Mg^{2+} was precipitated more easily in the form of $Mg(OH)_2$ as a separate phase. Moreover, the intensity of the peak corresponding to $CaMg(CO_3)_2$ and $CaZn(CO_3)_2$ was decreased with increasing the precipitation pH. It should be due to a competitive formation of hydroxide precipitates when the concentration of OH^- increased. At pH of 7, the

predominant species were CO_3^{2-}. Therefore, the metal carbonates should be formed with the higher amounts.
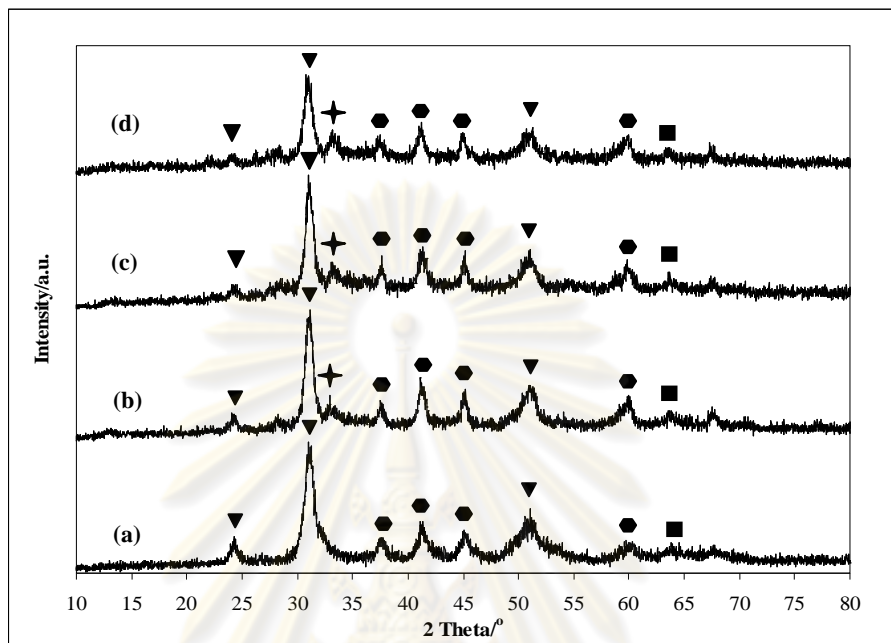
Figure 4.11 XRD patterns of as-synthesized CaMgZn111-II prepared at different pH: (a) 7, (b) 8, (c) 9 and (d) 10. (Symbols: (▼) $CaZn(CO_3)_2$, (⬟) $CaMg(CO_3)_2$, (■) $Zn(OH)_2$, and (✦) $Mg(OH)_2$

4.1.5 Effects of aging time and aging temperature

The effects of aging time and aging temperature on the elemental composition were investigated over CaMgZn catalyst with the metal ratio of 1:1:1, synthesized under the conditions II. As shown in Table 4.5, the aging time and the aging temperature did not affect the elemental composition of the resultant catalysts. It appeared that these three mixed oxides had a similar Ca:Mg:Zn molar ratio of 1:1:1.

Table 4.5 Elemental composition of calcined CaMgZn aged at different times and temperatures

Catalyst	Aging conditions	Ca:Mg:Zn molar ratio[a]		Metal composition in the solid (wt.%)		
		Mixture[b]	Solid[c]	CaO	MgO	ZnO
CaMgZn111-II	60 °C, 8 h	1:1:1	1:1:1	31.8	22.8	45.2
	60 °C, 20 h	1:1:1	1:1:1	32.9	17.8	49.3
	rt, 20 h	1:1:1	1:1:1	30.6	14.4	45.4

[a] Determined by XRF spectroscopy.

[b] Ca:Mg:Zn molar ratio in the synthesis mixture.

[c] Ca:Mg:Zn molar ratio in the final solid.

The influences of the aging conditions on the morphology of mixed precipitates before and after the calcination are illustrated in Figure 4.12a-4.12f. Aging the synthesis mixture at 60°C for 8 h resulted in CaMgZn precipitate with small spherical particles of 0.7-1 μm (Figure 4.12a). The particle size of CaMgZn precipitate was increased when the aging time was extended to 20 h as shown in Figure 4.12c (ca. 3 μm). It should be due to the aggregation of very small thin flake particles to form larger spheres. When CaMgZn precipitate was aged at room temperature for 20 h, the particle size was decreased to less than 0.5 μm (Figure 4.12e). It can be seen that the low aging temperature retarded the processes of precipitation of metal ions and the aggregation of precipitate nuclei, yielding uniform defect spheres. In all the cases, after the calcination, the particle sizes of resulting CaMgZn mixed oxides were smaller than those of the parent ones (Figure 4.12b, 4.12d and 4.12f), implying a considerable loss of CO_2 via the decarbonation. It is likely that these small spheres were derived from the decomposition of the aggregate thin flakes.
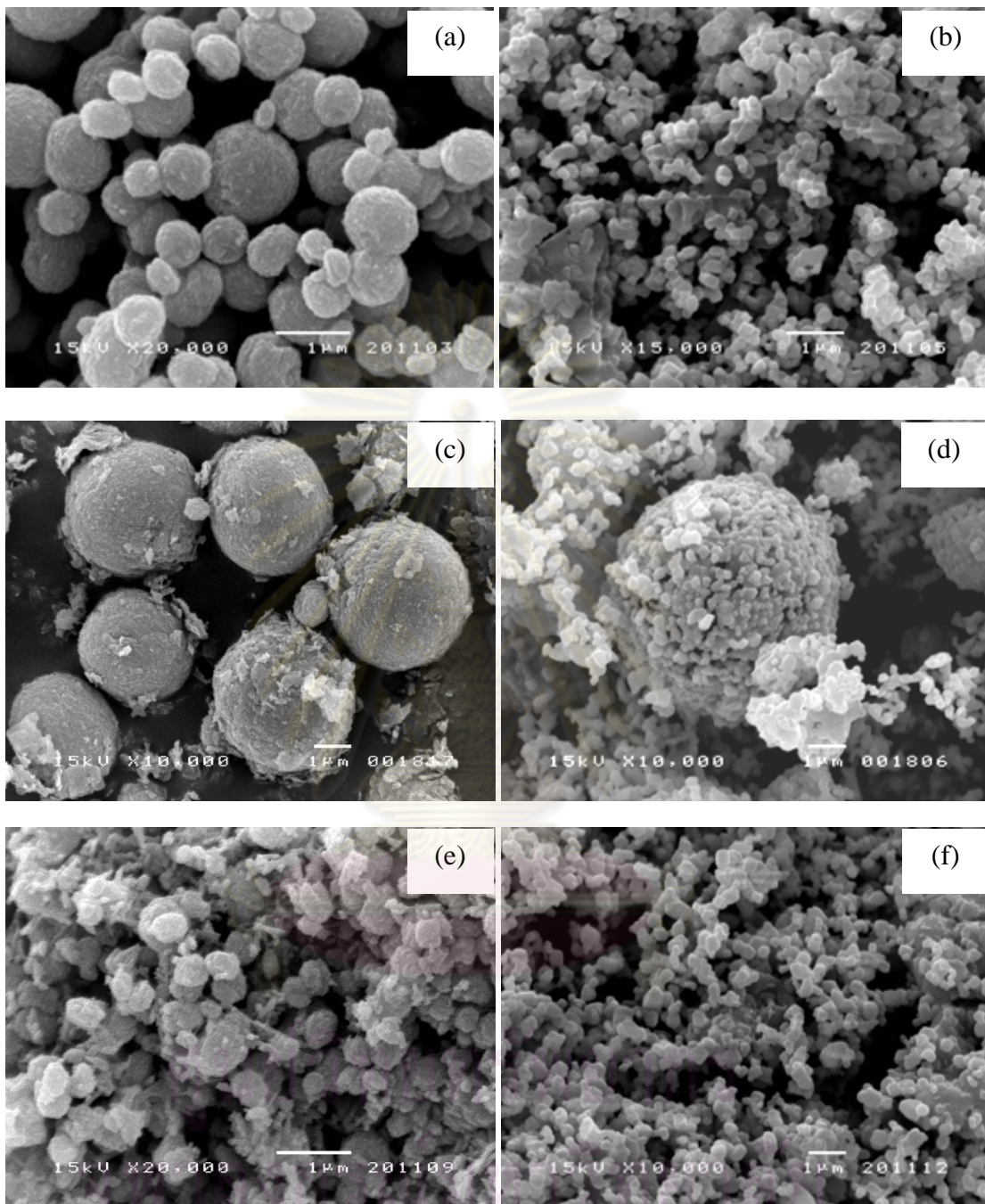
Figure 4.12 SEM images of CaMgZn precipitates aged at different times and temperatures

(a) uncalcined CaMgZn111-II (60°C, 8 h), (b) calcined CaMgZn111-II (60°C, 8 h),

(c) uncalcined CaMgZn111-II (60°C, 20 h), (d) calcined CaMgZn111-II (60°C, 20 h),

(e) uncalcined CaMgZn111-II (rt, 20 h), and (f) calcined CaMgZn111-II (rt, 20 h).

4.1.6 Effects of calcination temperature

The influence of calcination temperature, in the range of 500-800°C, on the morphology of catalyst was studied using SEM. For uncalcined sample (Figure 4.13a), it was found that the spherical particles were formed by an aggregation of small thin flake particles. After calcination, the merging of thin flake particles occurred. Increase of the calcination temperature from 500°C to 800°C caused an increase in the merging of thin flake particles (Figure 4.13b-4.13e).
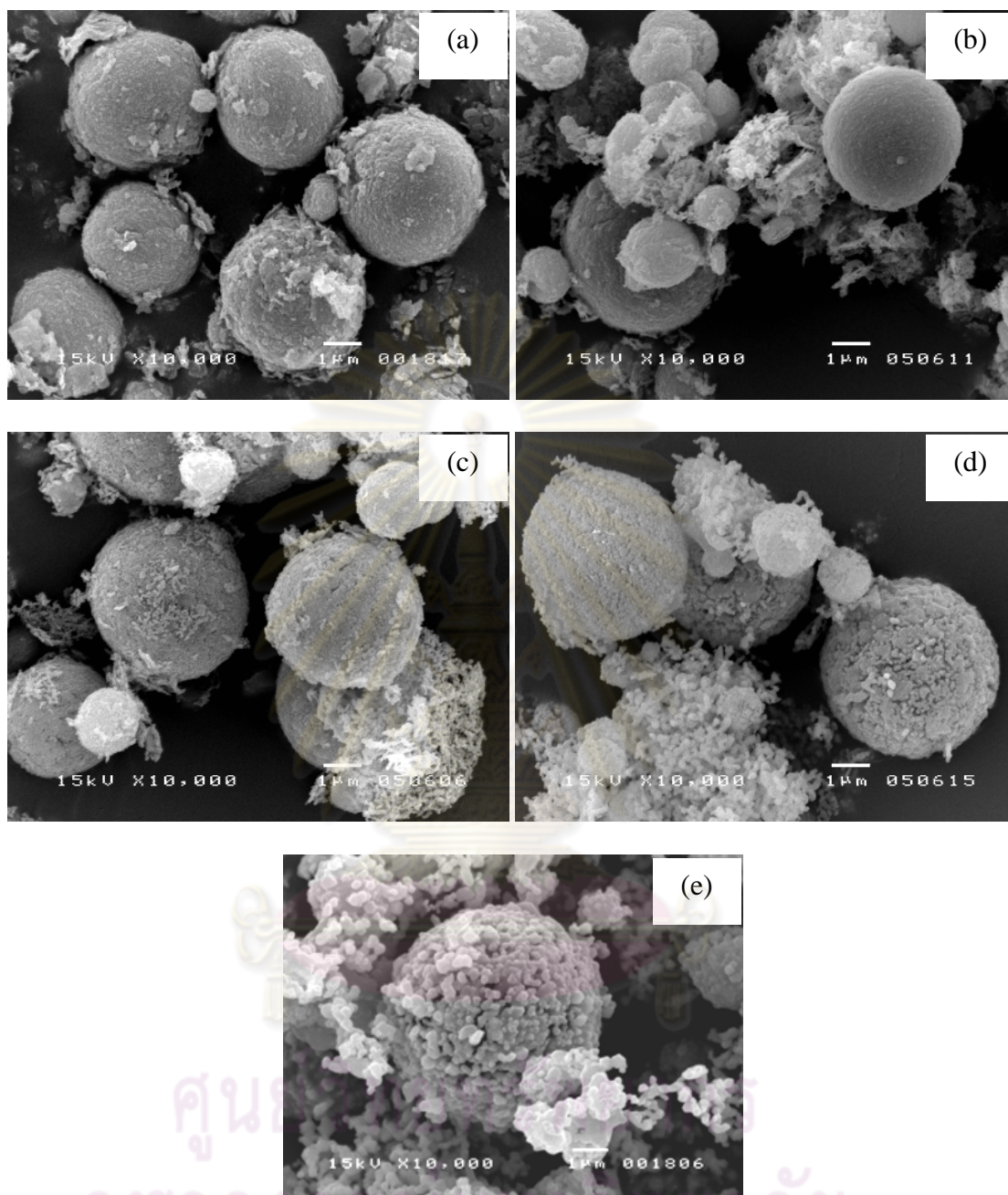
Figure 4.13 SEM images of CaMgZn111-II (a) before and after the calcinations at (b) 500°C, (c) 600°C, (d) 700°C**,** and (e) 800°C.

4.2 Transesterification over CaMgZn Catalysts

4.2.1 Effects of metal composition

The effect of metal composition on the palm kernel oil transesterification over different CaMgZn catalysts is shown in Table 4.6. It can be seen that the catalyst consisting of only Mg and Zn was not active for the formation of methyl esters. As discussed for the CO_2-TPD analysis results (Figure 4.8a), MgZn11-I showed the desorption peak at 237°C is attributed to the interaction of CO_2 with weak basic. The presence of weak basic sites resulted in the low activity for transesterification. With increasing the amount of Ca, CaMgZn311, the highest ME content of 98.0% can be attained. CaO is considered as the main basic sites responsible for the transesterification over the mixed oxides of CaZn [15], since it possesses the highest basicity ($H\_26.5$) [10]. It is interesting to note that an increase in the fraction of Mg (CaMgZn131) hampered the transesterification to larger extent than the case of Zn (CaMgZn113). Ngamcharussivichai et al. suggested that ZnO promoted the methyl ester synthesis over CaZn catalysts by reducing the particle size of the resultant mixed precipitates and facilitating the thermal decomposition of carbonate species to easily form the active CaO sites [15].

Table 4.6 Methyl esters (ME) content attained over calcined CaMgZn prepared with different Ca:Mg:Zn molar ratios

Catalyst	$\dfrac{Ca}{(Ca+Mg+Zn)}$	ME content (wt.%)
MgZn11-I	0	3.1
CaMgZn111-I	0.36	21.1
CaMgZn111-II	0.33	91.4
CaMgZn311-I	0.60	98.0
CaMgZn131-I	0.33	49.5
CaMgZn113-I	0.15	87.1

Transesterification conditions: catalyst amount, 6 wt%; methanol/oil molar ratio, 20; temperature, 60°C; time, 3 h.

Catalyst preparation condition I: CO_3^{2-}/metal molar ratio, 1; $[CO_3^{2-}]$, 0.75 M.

Catalyst preparation condition II: CO_3^{2-}/metal molar ratio, 1.5; $[CO_3^{2-}]$, 1.0 M.

To investigate the effect of catalyst preparation condition on the catalyst properties, the catalysts were prepared according to according to two different conditions: Condition I, the molar ratio of CO_3^{2-}/metal ion of 1, the CO_3^{2-} concentration of 0.75 M and Condition II, the molar ratio of CO_3^{2-}/metal ion of 1.5, the CO_3^{2-} concentration of 1.0 M.

The CO_2-TPD profiles of CaMgZn mixed oxides with different preparation conditions were shown in Figure 4.14. CaMgZn111-I and CaMgZn111-II showed a similar desorption profile (Figure 4.14a and 4.14b, respectively). The peaks located at 630°C and 717°C were ascribed to the desorption of CO_2 from the basic sites of CaO. CaMgZn111-II showed much higher peak intensity compared to CaMgZn111-I, which suggested CaMgZn111-II possesses high basicities, resulting in a high ME content (Table 4.6). Moreover, it was found that the desorption peak slightly shifted to the higher temperatures when compared to CaMgZn111-I.
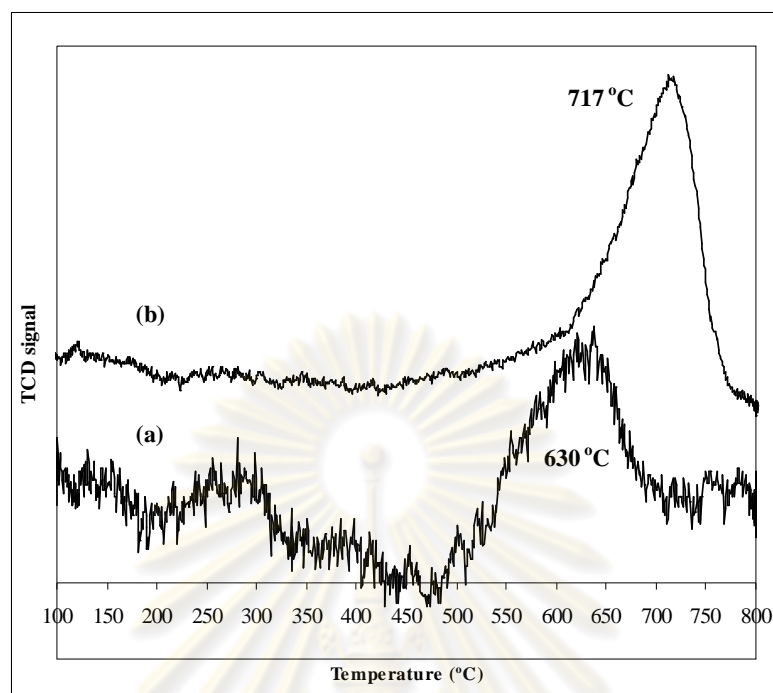
Figure 4.14 TPD analysis of CO_2 for calcined CaMgZn catalyst prepared with different preparation conditions : (a) CaMgZn111-I (the molar ratio of CO_3^{2-}/metal ion of 1, the CO_3^{2-} concentration of 0.75 M), and (b) CaMgZn111-II (the molar ratio of CO_3^{2-}/metal ion of 1.5, the CO_3^{2-} concentration of 1.0 M).

4.2.2 Effects of molar ratio of CO_3^{2-}/metal ion

Table 4.7 shows the effects of the molar ratio of CO_3^{2-}/metal ion on the ME content at the molar ratio of CO_3^{2-}/metal ion in the range of 0.75-1.5. It can be seen that, at the CO_3^{2-}/metal ion molar ratio of 0.75, the ME content attained was 8%. It should be related to an incomplete precipitation of metal ion at the low ratio, resulting in a low catalytic activity. As the molar ratio of CO_3^{2-}/metal ion was raised from 0.75 to 1.5, the ME content was increased and the highest ME content of 88.6% was obtained.

Table 4.7 Methyl esters (ME) content attained over calcined CaMgZn prepared with different molar ratios of CO_3^{2-}/metal ion

Catalyst	CO_3^{2-}/metal ion	$[CO_3^{2-}]$ (M)	$\dfrac{Ca}{(Ca+Mg+Zn)}$	ME content (wt.%)
CaMgZn111	0.75	0.5	0.44	8.0
	1.0	0.5	0.47	8.6
	1.5	0.5	0.37	88.6

Transesterification conditions: catalyst amount, 6 wt%; methanol/oil molar ratio, 20; temperature, 60°C; time, 3 h.

Catalyst preparation condition I: CO_3^{2-}/metal molar ratio, 1; $[CO_3^{2-}]$, 0.75 M.

Catalyst preparation condition II: CO_3^{2-}/metal molar ratio, 1.5; $[CO_3^{2-}]$, 1.0 M.

4.2.3 Effects of CO_3^{2-} concentration

To investigate the effects of CO_3^{2-} concentration on the formation of methyl esters, the catalysts were prepared by using the CO_3^{2-} concentration of 0.5 and 1.0 M. The results showed that when the CO_3^{2-} concentration was increased, the ME content was increased and the highest ME content (91.4%) was obtained at the CO_3^{2-} concentration of 1.0 M (Table 4.8). It should be related to the basicity of the catalysts.

Table 4.8 Methyl esters (ME) content attained over calcined CaMgZn prepared with different CO_3^{2-} concentrations

Catalyst	CO_3^{2-}/metal ion	$[CO_3^{2-}]$ (M)	$\dfrac{Ca}{(Ca+Mg+Zn)}$	ME content (wt.%)
CaMgZn111	1.5	0.5	0.37	88.6
	1.5	1.0	0.33	91.4

Transesterification conditions: catalyst amount, 6 wt%; methanol/oil molar ratio, 20; temperature, 60°C; time, 3 h.

4.2.4 Effects of pH during precipitation

In order to investigate the influences of pH during precipitation, the catalyst preparation was performed at various pH in the range of 7-10. From Table 4.9, it can be seen that the pH significantly affected the formation of methyl esters. The catalyst synthesized at pH 7 gave the highest ME content of 91.4%. At higher pH, the precipitation mechanism may be changed due to an increase in OH^-, resulting in the different mixed precipitate species. Consequently, the physicochemical properties of the resultant catalysts should be altered.

Table 4.9 Methyl esters (ME) content attained over calcined CaMgZn111-II mixed oxides prepared at different pH values

Catalyst	pH during precipitation	ME content (wt.%)
CaMgZn111-II	7	91.4
	8	80.2
	9	72.0
	10	5.1

Transesterification conditions: catalyst amount, 6 wt%; methanol/oil molar ratio, 20; temperature, 60°C; time, 3 h.

Catalyst preparation condition II: CO_3^{2-}/metal molar ratio, 1.5; $[CO_3^{2-}]$, 1.0 M.

4.2.5 Effects of aging time and aging temperature

The effects of aging time and aging temperature on the ME content were investigated over CaMgZn catalyst with the metal ratio of 1:1:1, synthesized under the conditions II (Table 4.10). It can be seen that the aging conditions did not only alter the morphology of the resultant mixed precipitate (Figure 4.12), but also affected the transesterification performance, and probably the basicity of mixed oxide as well. By combining the reaction results with the SEM analyses, it is likely that the calcined CaMgZn catalyst composed of smaller particle sizes was more active for the

formation of methyl esters. The defect spheres with uniform small size (Figure 4.12e-4.12f), obtained by aging at room temperature for 20 h, exhibited the highest ME content of 97.6%. Although aging at 60°C for 20 h resulted in the larger spherical particles formed by flake agglomerates (Figure 4.12c), the tiny particles appearing all over the spheres after the calcination (Figure 4.12d) catalyzed the reaction actively (91.4%). These results indicated that the aging time and the aging temperature are the important parameters for the preparation of CaMgZn mixed oxides for the transesterification.

Table 4.10 Methyl esters (ME) content attained over calcined CaMgZn111-II prepared under different aging conditions

Catalyst	Aging conditions	$\dfrac{Ca}{(Ca+Mg+Zn)}$	ME content (wt.%)
CaMgZn111-II	rt, 20 h	0.33	97.6
	60°C, 8 h	0.33	79.5
	60°C, 20 h	0.33	91.4

Transesterification conditions: catalyst amount, 6 wt%; methanol/oil molar ratio, 20; temperature, 60°C; time, 3 h.

Catalyst preparation condition II: CO_3^{2-}/metal molar ratio, 1.5; $[CO_3^{2-}]$, 1.0 M.

4.2.6 Effects of calcination temperature

The effect of calcination temperature for CaMgZn111-II on the transesterification was studied. The calcination temperatures varied from 500 - 800°C. As shown in Table 4.11, it can be seen that the calcination of mixed precipitates at 700 or 800°C increased the ME content > 90%, while the catalyst prepared from the mixed precipitates calcined at 500 or 600°C exhibited the ME content of only 3%. It should be due to an incomplete decomposition of $CaCO_3$ to CaO at low temperatures, resulting in the decrease in the transesterification activity. By combining the reaction results with the SEM analyses, it is likely that the calcined CaMgZn catalyst composed of smaller particle sizes was more active for the formation of methyl esters.

This result suggested that the calcination of mixed precipitates at 800°C provided the mixed oxides catalyst with high activity for the transesterification reaction.

Table 4.11 Methyl esters (ME) content attained over CaMgZn catalysts prepared under different calcination temperatures

Catalyst	Calcined temperature (°C)	ME content (wt.%)
CaMgZn111-II	500	3.0
	600	2.4
	700	90.0
	800	91.4

Transesterification conditions: catalyst amount, 6 wt%; methanol/oil molar ratio, 20; temperature, 60°C; time, 3 h.

Catalyst preparation condition II: CO_3^{2-}/metal molar ratio, 1.5; [CO_3^{2-}], 1.0 M.

4.2.7 Effects of catalyst amount

In order to determine the optimum reaction conditions, the influence of three parameters on palm kernel oil transesterification was examined: catalyst amount, methanol to oil molar ratio, and reaction time.

The influence of the catalyst amounts was studied at a 20:1 molar ratio of methanol to palm kernel oil at 60 °C for 3h. The catalyst amount was varied in the range of 2-8 wt.%. As shown in Figure 4.15, the methyl ester content was increased with the increase of catalyst amount from 2 to 6 wt.%. However, with further increase in the catalyst amount the methyl ester content was decreased, which was possibly due to a mixing problem involving reactants, products and solid catalyst.
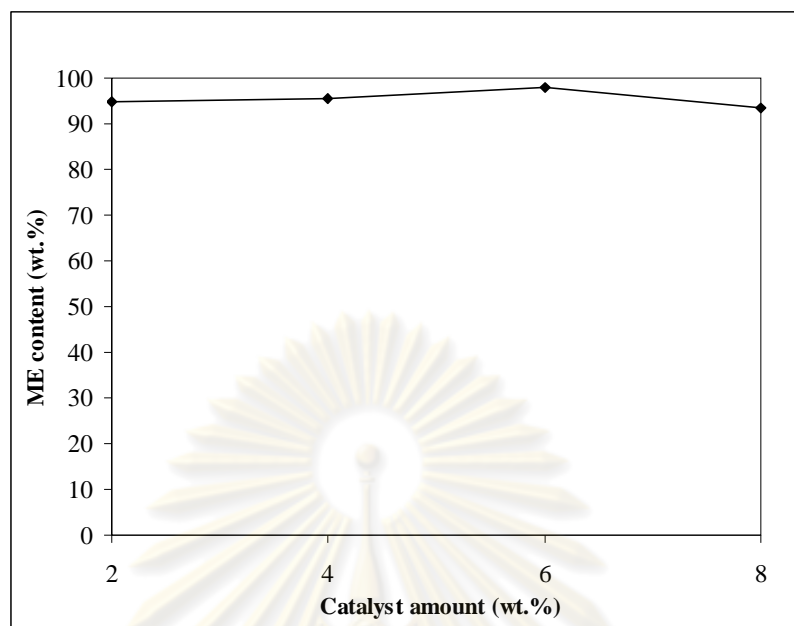
Figure 4.15 Dependence of methyl ester (ME) content on catalyst amount over CaMgZn311-I. Reaction conditions: methanol/oil molar ratio, 20:1; temperature, 60°C; time, 3 h.

4.2.8 Effects of molar ratio of methanol to oil

Stoichiometrically, the methanolysis of vegetable oil required three moles of methanol for each mole of oil. However, in practice, the molar ratio of methanol to oil should be higher than that of stoichiometric ratio in order to drive the reaction towards completion and produced more methyl ester as product. As shown in Figure 4.16, with an increase in the molar ratio of methanol to oil, the methyl ester content was increased considerably. The highest methyl content was obtained when the molar ratio was 20:1.

Figure 4.16 Dependence of methyl ester (ME) content on methanol/oil molar ratio over CaMgZn311-I. Reaction conditions: catalyst amount, 6 wt.%; temperature, 60°C; time, 3 h.

4.2.9 Effects of reaction time

The methyl ester content with various reaction times was shown in Figure 4.17. The reaction time was varied in the range 0.5-4 h. As can be seen from Figure 4.17, the methyl ester content was increased in the reaction time range between 0.5 and 2 h, and thereafter remained nearly constant as a result of near-equilibrium conversion; the maximum methyl ester content was achieved after 2h.
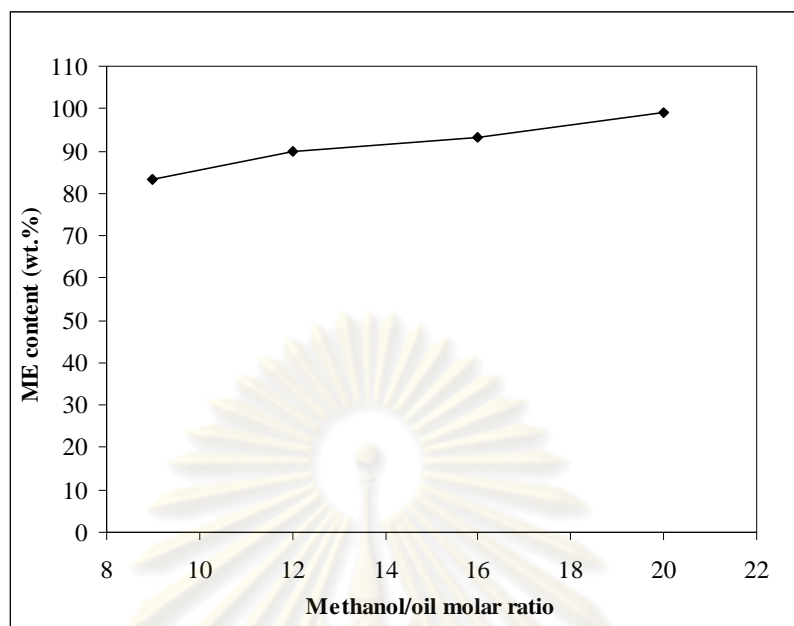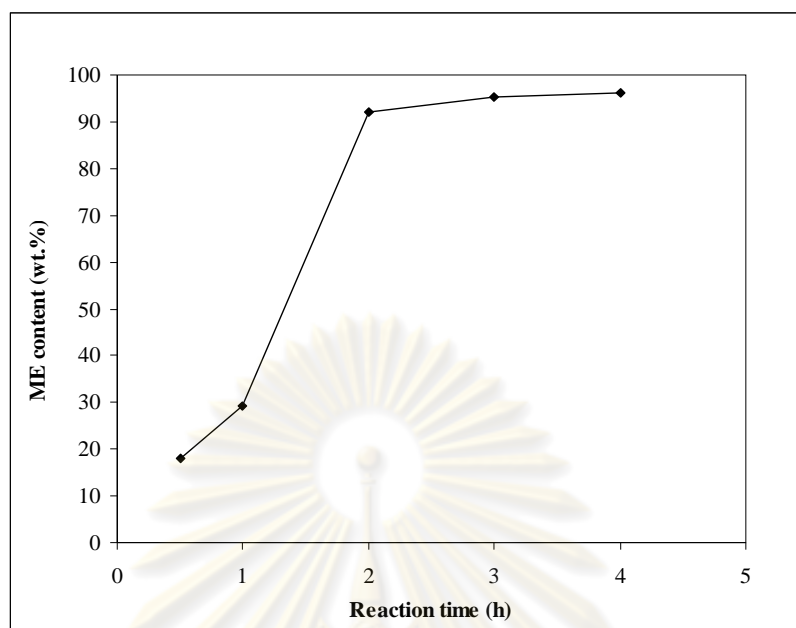
Figure 4.17 Dependence of methyl ester (ME) content on reaction time over CaMgZn311-I. Reaction conditions: catalyst amount, 6 wt.%; temperature, 60°C; methanol/oil molar ratio, 16

Table 4.12 Comparison of the activity of the prepared catalyst for transesterification of vegetable oils with the reported catalysts

Literature	Catalyst	Reactor	Catalyst amount (wt.%)	Alcohol/Oil molar ratio	Temperature (°C)	Time (h)	Yield (%)
Kim *et al*. [2]	Na/NaOH/γAl$_2$O$_3$	Autoclave	2	9:1 (MeOH : Soybean)	60°C	2	94.0
Benjapornkulaphong [78]	Ca(NO$_3$)$_2$/Al$_2$O$_3$	Flask	10	65:1 (MeOH : Palm kernel)	60°C	3	93.7
Liu *et al*. [10]	CaO	Flask	8	12:1 (MeOH : Soybean)	65°C	1.5	95.0
Albuquerque *et al*. [45]	MgCa mixed oxides	Flask	2.5	12:1 (MeOH : Sunflower)	100°C	1	92.0
Yan *et al*. [46]	ZnO-La$_2$O$_3$	Parr reactor	2.3	36:1 (MeOH : Waste oil)	200°C	3	92.0
Totarat [79]	CaZn mixed oxides	Flask	10	30:1 (MeOH : Palm kernel)	60°C	3	94.8
This research	CaMgZn mixed oxides	Flask	6	20:1 (MeOH : Palm kernel)	60°C	3	98.0

CHAPTER V

CONCLUSION AND RECOMMENDATIONS

5.1 Conclusion

In this thesis, the mixed oxides of Ca, Mg and Zn were prepared by pH-controlling co-precipitation of the corresponding metal nitrate salts and Na_2CO_3 solution. The characterizations of physicochemical properties of the synthesized materials were done by using techniques of X-ray diffraction, X-ray fluorescence spectrometry, scanning electron microscopy, thermogravimetric/differential thermal analysis, N_2 adsorption-desorption measurement and temperature-programmed desorption of CO_2. The catalytic performance of CaMgZn mixed oxides was evaluated in the transesterification of palm kernel oil with methanol. The following conclusions can be attained:

- The elemental analysis of the mixed oxides revealed that the precipitation of Mg^{2+} was low at low amount of CO_3^{2-}. Increasing the molar ratio of CO_3^{2-}/metal ion and the CO_3^{2-} concentration promoted the precipitation, yielding the desired Ca:Mg:Zn molar ratios.

- The XRD results indicated that the as-synthesized CaMgZn were precipitated in the form of mixed carbonates of CaMg and CaZn, and after the calcination the corresponding metal oxides were obtained.

- The as-synthesized CaMgZn morphologies showed the aggregation of small thin flakes to spherical particles with the size of 0.2-5.0 µm. The particle sizes of the spheres strongly depended on the aging time and aging temperature.

- The transesterification performance was largely influenced by the catalyst basicity, but not correlated with the amount of Ca containing in the catalyst.

- The CaMgZn catalyst synthesized at pH of 7 gave the highest ME content. At higher pH, the precipitation mechanism may be changed due to an increase in OH^-, resulting in the different mixed precipitate species.

- The highest methyl ester content of 98% was achieved over CaMgZn catalyst with the Ca:Mg:Zn molar ratio of 3:1:1, synthesized under the preparation conditions: the molar ratio of CO_3^{2-}/metal ion of 1.0, the CO_3^{2-} concentration of 0.75 M, the aging time of 20 h at 60°C.

- The suitable reaction conditions for the transesterification of palm kernel oil with methanol over the aforementioned CaMgZn311 were the methanol/oil molar ratio of 20, the amount of catalyst of 6 wt.%, the reaction time of 3 h, and the temperature of 60°C.

5.2 Recommendations

For future work, the catalyst preparation should be investigated in detail, for example:
- To study the precipitation mechanism of mixed carbonates.
- To study the interaction of metals in mixed carbonates and oxides by X-ray photoelectron spectroscopy (XPS).

REFERENCES

[1]   Ma, F.; and Hanna, M.A. Biodiesel production: a review. **Bioresource Technolnology** 70 (1999): 1-15.

[2]   Kim, H. J.; Kang, B.S.; Kim, M.J.; Park, Y.M.; Kim, D.K.; Lee, J.S.; and Lee, K.Y. Transesterification of vegetable oil to biodiesel using heterogeneous base catalyst. **Catalysis Today** 93-95 (2004): 315-320.

[3]   Ebiura, T.; Echizen, T; Ishikawa, A.; Murai, K.; and Baba, T. Selective transesterification of triolein with methanol to methyl oleate and glycerol using alumina loaded with alkali metal salt as a solid-base catalyst. **Applied Catalysis A: General** 283 (2005): 111-116.

[4]   Xie, W.; Peng, H.; and Chen, L. Transesterification of soybean oil catalyzed by potassium loaded on alumina as a solid-base catalyst. **Applied Catalysis A: General** 300 (2006): 67-74.

[5]   Xie, W.; and Li, H. Alumina supported potassium iodide as a heterogeneous catalyst for biodiesel production from soybean oil. **Journal of Molecular Catalysis** 255 (2006): 1-9.

[6]   Alonso, D.M.; Mariscal, R.; Tost, R.M.; Poves, M.D.Z.; and Granados, M.L. Potassium leaching during triglyceride transesterification using K/ γ-Al$_2$O$_3$ catalysts. **Catalysis Communication** 8 (2007): 2080-2086.

[7]   Gryglewicz, S. Rapeseed oil methyl esters preparation using heterogeneous catalysts. **Bioresource Technology** 70 (1999): 249-253.

[8]   Reddy, C.; Reddy, V.; Oshel, R.; and Verkade, J.G. Room-temperature conversion of soybean oil and poultry fat to biodiesel catalyzed by nanocrystalline calcium oxides. **Energy & Fuel** 20 (2006): 1310-1314.

[9]   Granados, M.L.; Poves, M.D.Z.; Alonso, D.M.; Mariscal, R.; Galisteo, F.B.; Tost, R.M.; Santamaria, J.; and Fierro, J.L.G. Biodiesel from sunflower oil by using activated calcium oxide. **Applied Catalysis B: Environmental** 73 (2007):317-326.

[10]   Liu, X.; He, H.; Wang, Y.; Zhu, S.; and Piao, X. Transesterification of soybean oil to biodiesel using CaO as a solid base catalyst. **Fuel** 87 (2008): 216-221.

[11]   Kouzu, M.; Kasuno, T.; Tajika, M.; Sugimoto, Y.; Yamanaka, S.; and Hidaka, J. Calcium oxide as a solid base catalyst for transesterification of soybean oil and its application to biodiesel production. **Fuel** 87 (2008): 2798-2806.

[12]   Cantrell, D.G.; Gillie, L.J.; Lee, A.F.; and Wilson, K. Structure-reactivity correlations in MgAl hydrotalcite catalysts for biodiesel synthesis. **Applied Catalysis A: General** 287 (2005): 183-190.

[13]   Serio, M.D.; Ledda, M.; Cozzolina, M.; Minutillo, G.; Tesser, R.; and Santacesaria, E. Transesterification of soybean oil to biodiesel by using heterogeneous basic catalysts. **Industrial & Engineering Chemistry Research** 45 (2006): 3009-3014.

[14]   Shumaker, J.L.; Crofcheck, C.; Tackett, S.A.; Santillan-Jimenez, E.; and Crocker, M. Biodiesel production from soybean oil using calcined Li-Al layered double hydroxide catalysts. **Catalysis Letters** 115(2007): 56-61

[15]   Ngamcharussrivichai, C.; Totarat, P.; and Bunyakiat, K. Ca and Zn mixed oxide as a heterogeneous base catalyst for transesterification of palm kernel oil. **Applied Catalysis A: General** 341(2008): 77-85.

[16]   Joshi, R.M.; and Pegg, M.J. Flow properties of biodiesel fuel blends at low temperatures. **Fuel** 86 (2007): 143-157.

[17]   Department of Energy Business, Ministry of Energy, Thailand. **Standard specification for biodiesel in Thailand** [Online] Available from: http://www.doeb.go.th [2009, June 1]

[18]   Bahadur, N.P.; Boocock, D.G.B.; and Konar, S.K. Liquid hydrocarbons from catalytic pyrolysis of sewage sludge lipid and canola oil: evaluation of fuel properties. **Energy & Fuel** 9(1995): 248-256.

[19]   Ali, Y.; Hanna, M.A.; and Cuppett, S.L. Fuel properties of tallow and soybean oil esters. **Journal of the American Oil Chemists' Society** 72(1995): 1557-1564.

[20] Canakci, M.; and Sanli, H. Biodiesel production from various feedstocks and their effects on the fuel properties. **Journal of Industrial Microbiology and Biotechnology** 35(2008): 431-441.

[21] Knothe, G. Dependence of biodiesel fuel properties on the structure of fatty acid alkyl esters. **Fuel Processing Technology** 86(2005): 1059-1070.

[22] Mittelbach, M. Diesel fuel derived from vegetable oils, VI: specifications and quality control of biodiesel. **Bioresource Technolnology** 56(1996): 7-11.

[23] Song, C.; Hsu, C.S.; and Mochida, I. **Chemistry of Diesel Fuels** New York: Taylor & Francis, 2000.

[24] Demirbas, A. Characterization of biodiesel fuels. **Energy Sources, Part A: Recovery, Utilization, and Environmental Effects** 31 (2009): 889-896.

[25] Monyem, A.; and Gerpen, J.H.V. The effect of biodiesel oxidation on engine performance and emissions. **Biomass and Bioenergy** 20(2001): 317-325.

[26] Formo, M.W.; Jungerman, E.; Norris, F.A.; and Sonntag, N.O.V. **Bailey's industrial oil and fat products 4th ed** New York: John Weiley and son, 1979.

[27] Ramos, M.J.; Fernandez, C.M.; Casas, A.; Rodriguez, L.; and Perez, A. Influence of fatty acid composition of raw materials on biodiesel properties. **Bioresource Technolnology** 100(2009): 261-268.

[28] Moser, B.R. Biodiesel production, properties, and feedstocks. **In Vitro Cellular & Developmental Biology - Plant** 45(2009): 229-266.

[29] Demirbas, A. Biodiesel fuels from vegetable oils via catalytic and non catalytic supercritical alcohol transesterifications and other methods: a survey. **Energy Conversion and Management** 44(2003): 2093-2109.

[30] Barnwal, B.K.; and Sharma, M.P. Prospects of biodiesel production from vegetable oils in India. **Renewable and Sustainable Energy Reviews** 9(2005): 363-378.

[31] Tiwari A.K.; Kumar, A.; and Raheman, H. Biodiesel production from jatropha oil (*Jatropha curcus*) with high free fatty acids: an optimized process. **Biomass and Bioenergy** 31(2007): 569-575.

[32] Shama, Y.C.; and Singh, B. Development of biodiesel from karanja, a tree found in rural India. **Fuel** 67(2008): 1740-1742.

[33] Pleanjai, S; and Gheewala, S.H. Full chain energy analysis of biodiesel production from palm oil in Thailand. **Applied Energy** 86 (2009): S209-S214

[34] Gunstone, F.D. **Vegetable oils in food technology: composition, properties, and uses** Oxford: Blackwell, 2002.

[35] Demirbas, A. Progress and recent trends in biodiesel fuels. **Energy Conversion and Management** 50(2009):14-34

[36] Sanli, H.; and Canakci, M. Effects of different alcohol and catalyst usage on biodiesel production from different vegetable oils. **Energy & Fuel** 22(2008): 2713-2719.

[37] Kulkarni, M.G.; and Dalai, A.K. Waste cooking oil-an economical source for biodiesel: A review. **Industrial & Engineering Chemistry Research** 45(2006): 2901-2913.

[38] Schuchardi, U.; Sercheli, R.; and Vargas, R.M. Transesterification of vegetable oils: a review. **Journal of the Brazilian Chemical Society** 9(1998): 199-210.

[39] Helwani, Z.; Othman, M.R.; Aziz, N.; Kim, J.; and Fernando, W.J.N. Solid heterogeneous catalysts for transesterification of triglycerides with methanol: A review. **Applied Catalysis A: General** 363(2009): 1-10.

[40] Boz, N.; and Kara, M. Solid base catalyzed transesterification of canola oil. **Chemical Engineering Communications** 196(2009): 80-92.

[41] Noiroj, K.; Intarapong, P.; Luengnaruemitchai, A.; and Jai-In, S. A comparative study of KOH/Al_2O_3 and KOH/NaY catalysts for biodiesel production via transesterification from palm oil. **Renewable Energy** 34(2009): 1145-1150.

[42] Hattori, H. Heterogeneous basic catalysis. **Chemical Reviews** 95(1995): 537-558.

[43] Zeng, H. Y.; Feng, Z.; Deng, X.; and Li, Y. Q. Activation of Mg-Al hydrotalcite catalysts for transesterification of rape oil. **Fuel** 87(2008): 3071-3076.

[44]   Babu, N.S.; Sree, R.; Prasad, P.S.S.; and Lingaiah, N. Room-temperature transesterification of edible and nonedible oils using a heterogeneous strong basic Mg/La catalyst. **Energy & Fuel** 22(2008): 1965-1971.

[45]   Albuquerque, M.C.G.; Santamaría-González, S.; Mérida-Robles, J.M.; Moreno-Tost,R.; Rodríguez-Castellón, E.; Jiménez-López, A.; Azevedo, D.C.S.; Cavalcante Jr, C.L.; and Maireles-Torres, P. MgM (M = Al and Ca) oxides as basic catalysts in transesterification processes. **Applied Catalysis A: General** 347(2008):162-168

[46]   Yan, S.; Salley, S.O.; and Simon, K.Y. Simultaneous transesterification and esterification of unrefined or waste oils over $ZnO-La_2O_3$ catalysts. **Applied Catalysis A: General** 353(2009): 203-212.

[47]   Lotero, E.; Liu, Y.; Lopez, D.E.; Suwannakarn, K.; Bruce, D.A. and Goodwin, J.G. Synthesis of biodiesel via acid catalysis. **Industrial & Engineering Chemistry Research** 44(2005): 5353-5363.

[48]   Brito, A.; Borges, M.E.; and Otero, N. Zeolite Y as a heterogeneous catalyst in biodiesel fuel production from used vegetable oil. **Energy & Fuel** 21(2007): 3280-3283.

[49]   Morin, P.; Hamad, B.; Sapaly, G.; Rocha, M.G.C.; Pries de Oliviera, P.G.; Gonzalez, W.A.; Sales, E.A.; and Essayem, N. transesterification of rapeseed oil with ethanol I. Catalysis with homogeneous Keggin heteropolyacids. **Applied Catalysis A: General** 330(2007): 69-76.

[50]   Kulkarni, M.G.; Gopinath, R.; Meher, L.C.; and Dalai, A.K. Solid acid catalyzed biodiesel production by simultaneous esterification and transesterification. **Green Chemistry** 8(2006): 1056-1062.

[51]   Jitputti, J.; Kitiyanan, B.; Rangsunvigit, P.; Bunyakiat, K.; Attanatho, L.; and Jenvanitpanjakul, P. Transesterification of crude palm kernel oil and crude coconut oil by different solid catlysts. **Chemical Engineering Journal** 116(2006): 61-66.

[52]   Kiss, A. A.; Omota, F.; Dimian, A.C.; and Rothenberg, G. The heterogeneous advantage: biodiesel by catalytic reactive distillation. **Topics in Catalysis** 40(2006): 141-150.

[53] Lopez, D.E.; Goodwin, J.G.; Bruce, D.A. Transesterification of triacetin with methanol on nafion acid resins. **Journal of Catalysis** 245(2007): 381-191.

[54] Mbaraka, I.; and Shanks, B.H. Conversion of oils and fats using advanced mesoporous heterogeneous catalysts. **Journal of the American Oil Chemists' Society** 83(2006): 79-91.

[55] Antczak, M. S.; Kubiak, A.; Antczak, T.; and Bielecki, S. Enzymatic biodiesel synthesis - Key factors affecting efficiency of the process. **Renewable Energy** 34(2009): 1185-1194.

[56] Medina, A.R.; Moreno, P.A.G.; Cerdan, E.; and Grima, E.M. Biocatalysis: Towards ever greener biodiesel production. **Biotechnology Advances** 27(2009): 398-408.

[57] Watanabe, Y.; Shimada, Y.; Sugihara, A.; Noda, H.; Fukada, H.; and Tominaga, Y. Continuous production of biodiesel fuel from vegetable oil using immobilized *Candida antartica* lipase. **Journal of the American Oil Chemists' Society** 77(2000): 355-360.

[58] Watanabe, Y.; Shimada, Y.; Sugihara, A.; and Tominaga, Y. Conversion of degummed soybean oil to biodiesel fuel with immobilized *Candida Antarctica* lipase. **Journal of Molecular Catalysis B: Enzymatic** 17(2002): 151-155.

[59] Linko, Y.Y.; Lamsa, M.; Wu, X.; Uosukainen, E.; Seppala, J.; and Linko, P. Biodegradable products by lipase biocatalysis. **Journal of Biotechnology** 66(1998): 41-50.

[60] Ghanem, A. The utility of cyclodextrins in lipase-catalyzed transesterification in organic solvents: enhanced reaction rate and enantioselectivity. **Organic and Biomolecular Chemistry** 1(2003): 1282-1291.

[61] Dossat, V.; Combes, D.; and Marty, A. Continuous enzymatic transesterification of high oleic sunflower oil in a packet bed reactor: influence of the glycerol production. **Enzyme and Microbial Technology** 25(1999): 194-200.

[62] Iso, M.; Chen, B.; Eguchi, M.; Kudo, T.; and Shrestha, S. Production of biodiesel fuel from triglycerides and alcohol using immobilized lipase. **Journal of Molecular Catalysis B: Enzymatic** 16(2001): 53-58.

[63]   Xu, Y.; Du, W.; Liu, D. ; and Zeng, J. A novel enzymatic route for biodiesel production from renewable oils in a solvent-free medium. **Biotechnology Letters** 25(2003): 1239-1241.

[64]   Campanati, M.; Fornasari, G.; and Vaccari, A. Fundamentals in the preparation of heterogeneous catalysts. **Catalysis Today** 77(2003): 299-314.

[65]   Schwarz, J.A.; Contescu, C.; and Contescu A. Methods for preparation of catalytic materials. **Chemical Reviews** 95(1995): 477-510.

[66]   Etrl, G.; Knözinger, H.; and Weitkamp, J. **Preparation of solid catalysts** New York: Wiley VCH, 1999.

[67]   Hendrick, D.W. **Water treatment unit process: physical and chemical** New York: Taylor & Francis, 2005

[68]   Tittabut, T. and Trakarnpruk, W. Metal-Loaded MgAl oxides for transesterification of glyceryl tributyrate and palm oil. **Industrial & Engineering Chemistry Research** 47(2008): 2176-2181.

[69]   Chuayplod, P. and Trakarnpruk, W. Transesterification of rice bran oil with methanol catalyzed by Mg(Al)La hydrotalcites and Metal/MgAl oxides. **Industrial & Engineering Chemistry Research** 48(2009): 4177-4183.

[70]   Albuquerque, M.C.G.; Azevedo, D.C.S.; Cavalcante Jr, C.L.; Santamaría-González, J.; Mérida-Robles, J.M.; Moreno-Tost, R.; Rodríguez-Castellón, E.; Jiménez-López, A.; and Maireles-Torres, P. Transesterification of ethyl butyrate with methanol using MgO/CaO catalysts. **Applied Catalysis A: General** 300(2009): 19-24.

[71]   Chorkendorff, I.; and Niemantsverdriet, J.W. **Concepts of modern catalysis and kinetics** New York: Wiley VCH, 2003.

[72]   BET   Surface   Area   [Online].   Available   from: http://en.wikipedia.org/wiki/BET_theory [2009, July 1]

[73]   Basic   Theory   of   X-ray   Fluorescence   [online].   Available   from: http://www.learnxrf.com/BasicXRFTheory.html [2009, July 1]

[74]   Thermogravimetric   analysis   [online].   Available   from: http://en.wikipedia.org/wiki/Thermogravimetric_analysis [2009, July 1]

[75] Differential thermal analysis [online]. Available from: http://en.wikipedia.org/wiki/Differential_thermal_analysis [2009, July 1]

[76] Boaro, M.; Vicario, M.; de Leitenburg, C.; Dolcetti, G.; and Trovarelli, A. The use of temperature-programmed and dynamic/transient methods in catalysis: characterization of ceria-based, model three-way catalysts. **Catalysis Today** 77(2003): 407-417.

[77] Sawada, Y.; Murakami, M.; and Nishide, T. Thermal analysis of basic zinc carbonate. Part 1. Carbonation process of zinc oxide powders at 8 and 13°C. **Thermochimica Acta** 273 (1996): 95-102.

[78] Benjapornkulaphong, S. **Heterogeneous catalytic transesterifation of palm kernel oil and coconut oil** Master's Thesis, Department of Chemical Technology, Faculty of Science, Chulalongkorn University, 2005.

[79] Totarat, P. **Transesterification of vegetable oil over basic mixed oxide catalysts** Master's Thesis, Department of Chemical Technology, Faculty of Science, Chulalongkorn University, 2007.

APPENDICES

Appendix A

Calculation for Catalyst Preparation

Table A-1 Molecular weight of chemical used in the catalyst preparation

Chemical	Molecular weight (g mol^{-1})
$Ca(NO_3)_2 .4H_2O$	236.15
$Mg(NO_3)_2.6H_2O$	256.41
$Zn(NO_3)_2.6H_2O$	297.47
Na_2CO_3	106

The amount of chemical used in the catalyst preparation was calculated as follows:

Example Preparation of CaMgZn mixed oxides with the Ca:Mg:Zn molar ratio of 1:1:1 (CO_3^{2-}/metal ion molar ratio of 1.5 and CO_3^{2-} concentration of 1 M).

(1) Calculation for the preparation of metal solution (Ca:Mg:Zn = 1:1:1)

0.02 mol of $Ca(NO_3)_2 .4H_2O$ = 0.02 x 236.15 = 4.723 g

0.02 mol of $Mg(NO_3)_2.6H_2O$ = 0.02 x 256.41 = 5.13 g

0.02 mol of $Zn(NO_3)_2.6H_2O$ = 0.02 x 297.47 = 5.95 g

Therefore, 4.723 g of $Ca(NO_3)_2 .4H_2O$, 5.13 g of $Mg(NO_3)_2.6H_2O$, and 5.95 g of $Zn(NO_3)_2.6H_2O$ were dissolved in 200 ml of deionized water.

(2) Calculation for the preparation of Na_2CO_3 solution

From the CO_3^{2-}/metal ion molar ratio of 1.5

Mol of metal = 0.02 + 0.02 + 0.02 = 0.06

Therefore, Mol of CO_3^{2-} = 1.5 x 0.06 = 0.09

Calculate the volume of 1M Na_2CO_3 solution required to prepare catalyst

From mol = cv/1000

where c is the concentration, and v is the volume.

The Na$_2$CO$_3$ solution volume = $\dfrac{\text{Mol of CO}_3^{2-} \times 1000}{\text{CO}_3^{2-} \text{ concentration}}$

$= \dfrac{0.09 \times 1000}{1}$ = 90 ml

ศูนย์วิทยทรัพยากร

จุฬาลงกรณ์มหาวิทยาลัย

Appendix B

Fatty Acid Composition of Palm Kernel Oil

Table B-1 Fatty acid composition of palm kernel oil used in the present study

Fatty acid	Symbol	Fatty composition (wt.%)
Caproic acid	C 6:0	0.24
Capryric acid	C 8:0	5.14
Capric acid	C 10:0	4.82
Lauric acid	C 12:0	59.83
Myristic acid	C 14:0	14.92
Palmitic acid	C 16:0	5.38
Stearic acid	C 18:0	1.52
Saturated		**91.85**
Oleic acid	C 18:1	6.87
Linoleic acid	C 18:2	1.28
Unsaturated		**8.15**
Total fatty acid composition		100
Molecular weight		677.60

Appendix C

Calculation of Methyl Ester Content

n-heptane

2 —

Methyl caprylate (C8:0)

Methyl caprate (C10:0)

Methyl undecanoate (C11:0)

4 —

Methyl laurate (C12:0)

6 —

Methyl myristate (C14:0)

8 —

Methyl palmitate (C16:0)

10 —

12 — **Methyl linoleate (C18:2)**

Methyl oleate (C18:1)
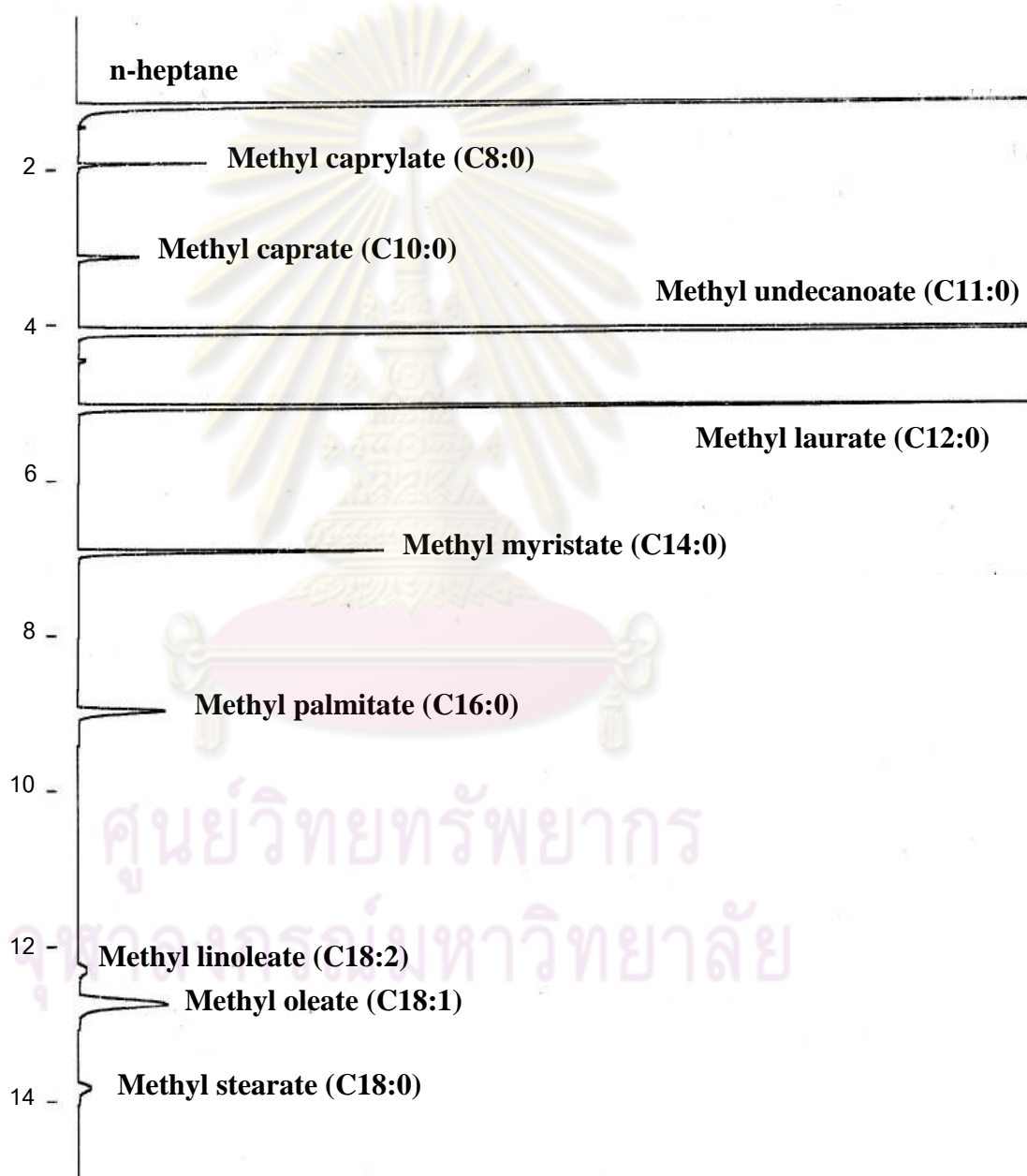
14 — **Methyl stearate (C18:0)**

Figure C-1 Gas chromatogram of methyl ester product

The methyl ester content (wt.%) was calculate from the formula

$$\text{wt.\%} = (\sum A_i \times W_{Std})/(A_{Std} \times W_S)$$

Where $\sum A_i$ = The total area from methyl ester, from methyl caprylate (C8:0) to methyl stearate (C18:0)

W_{Std} = The weight of methyl undecanoate

A_{Std} = The area of methyl undecanoate

W_S = The weight of the sample

Appendix D

Calculation of Methanol to Oil Molar Ratio

Example Calculation of methanol to oil molar ratio of 20

Molecular weight of palm kernel oil	=	677.60 g mol^{-1}
Density of palm kernel oil	=	0.922 g ml^{-1}
Molecular weight of methanol	=	32.04 g mol^{-1}
Density of methanol	=	0.792 g ml^{-1}

For 10 g of palm kernel oil

From molecular weight of palm kernel oil = 677.60 g

So, 10 g of palm kernel oil = 10/677.6 = 0.0148 mol

From methanol to oil molar ratio of 20

So, mol of methanol = 20 x 0.0148 = 0.296 mol

From molecular weight of methanol = 32.04 g mol^{-1}

So, methanol = 0.296 x 32.04 = 9.48 g

From density of methanol = 0.792 g ml^{-1}

So, methanol = 9.48/0.792 = 12 ml

Therefore, the desired amount of methanol was 12 ml.

VITA

Miss Sasipim Limmanee was born on January 21, 1985 in Trang, Thailand. She graduated with a Bachelor's degree of Science, majoring in Chemistry, Faculty of Science, Mahidol University in 2007. She has continued her study in Master's degree, majoring in Petrochemistry and Polymer Science, Faculty of Science, Chulalongkorn University, Bangkok, Thailand since 2007 and finished her study in 2009.

Oral presentation for the Pure and Applied Chemistry Conference (PACCON 2009) which organized by Naresuan University in the topic of "Ca, Mg AND Zn MIXED OXIDES AS HETEROGENEOUS BASE CATALYSTS FOR TRANSESTERIFICATION OF VEGETABLE OILS"